Targeting HECTD3-IKKα axis inhibits inflammation-related metastasis

CeShi Chen (chenc@mail.kiz.ac.cn)
Kunming Institute of Zoology, CAS

Fubing Li
Kunming Institute of Zoology, Chinese Academy of Sciences

Huichun Liang
Kunming Institute of Zoology, Chinese Academy of Sciences

Hua You
Guangzhou Medical University

Ji Xiao
Medical Faculty of Kunming University of Science and Technology

Hou-Jun Xia
Kunming Institute of Zoology https://orcid.org/0000-0003-1045-1465

Xi Chen
Key Laboratory of Animal Models and Human Disease Mechanisms of Chinese Academy of Sciences & Yunnan Province, Kunming Institute of Zoology, Kunming, Yunnan 650223, China

Maobo Huang
Key Laboratory of Animal Models and Human Disease Mechanisms of Chinese Academy of Sciences & Yunnan Province, Kunming Institute of Zoology, Kunming, Yunnan 650223, China

Zhuo Cheng
Key Laboratory of Animal Models and Human Disease Mechanisms of Chinese Academy of Sciences & Yunnan Province, Kunming Institute of Zoology, Kunming, Yunnan 650223, China

Chuanyu Yang
Kunming Institute of Zoology, Chinese Academy of Sciences

Wenjing Liu
Key Laboratory of Animal Models and Human Disease Mechanisms of Chinese Academy of Sciences & Yunnan Province, Kunming Institute of Zoology, Kunming, Yunnan 650223, China

Hai-Lin Zhang
Kunming Institute of Zoology

Li Zeng
Key Laboratory of Animal Models and Human Disease Mechanisms of Chinese Academy of Sciences & Yunnan Province, Kunming Institute of Zoology, Kunming, Yunnan 650223, China

Yingying Wu
Kunming Medical University

Fei Ge
Kunming Institute of Zoology
Zhen Li
Kunming Medical University
Wenhui Zhou
Hubei University of Medicine
Zhongmei Zhou
Kunming Institute of Zoology
Rong Liu
Key Laboratory of Animal Models and Human Disease Mechanisms of Chinese Academy of Sciences & Yunnan Province, Kunming Institute of Zoology, Kunming, Yunnan 650223, China
Dewei Jiang
Kunming Institute of Zoology
Yi Wen
Key Laboratory of Animal Models and Human Disease Mechanisms of Chinese Academy of Sciences & Yunnan Province, Kunming Institute of Zoology, Kunming, Yunnan 650223, China
Ni Xie
Shenzhen University
Yanjie Kong
Shenzhen University
Bin Liang
Yunnan University https://orcid.org/0000-0001-9131-5478

Article

Keywords: HECTD3, Ubiquitination, IKKα, Metastasis, NF-κB

Posted Date: January 7th, 2021

DOI: https://doi.org/10.21203/rs.3.rs-130038/v1

Abstract

Metastasis is the leading cause of cancer-related death. Surgery is a common intervention for most primary solid tumors; however, surgical trauma-related systemic inflammation facilitates distant tumor metastasis by increasing the spread and adhesion of tumor cells to vascular endothelial cells. Currently, there are no effective interventions to prevent distant metastasis. Here, we show that HECTD3 deficiency in vascular endothelial cells (ECs) significantly reduces tumor metastasis in tumor resection metastasis, LPS-induced metastasis and *MMTV-Neu* metastasis models. HECTD3 depletion downregulates expression of adhesion molecules, such as VCAM-1, ICAM-1 and E-selectin, in mouse primary ECs and in human primary umbilical vein ECs stimulated by inflammatory factors and inhibits adhesion of tumor cells to ECs both *in vitro* and *in vivo*. We demonstrate that HECTD3 promotes stabilization and kinase activity of IKKα by ubiquitinating IKKα with K27- and K63-linked polyubiquitin chains at K296, increasing phosphorylation of histone H3 at Ser10 to promote NF-κB target gene transcription. IKKα kinase inhibitors prevented LPS-induced pulmonary metastasis. These findings reveal the promotional role of the HECTD3-IKKα axis in tumor hematogenous metastasis and provide a potential strategy for tumor metastasis prevention.

Introduction

Metastasis accounts for 90% of deaths in cancer patients [1]. Cancer patients without clinical symptoms after initial treatment frequently develop distant metastasis years later [2]. Surgery is a common early intervention for most solid tumors. However, mechanical trauma and the subsequent wound healing process constitute favorable factors for metastases through several mechanisms, including release of circulating tumor cells (CTCs) [3,4] and triggering systemic inflammation [5,6]. To avoid anoikis during metastasis, CTCs must attach to the vasculature of distant organs and extravasate into the perivascular tissue.

Accumulating data indicate that systemic inflammation potentiates the adhesion of CTCs to vascular endothelial cells (ECs) of distant organs. This is a key step of extravasation in hematogenous metastasis [5,6]. CTC extravasation typically occurs in small capillaries [7,8], where cancer cells are arrested by the endothelium via interaction with a wide range of adhesion molecules of ECs, including E-selectin, ICAM-1 (intercellular-adhesion molecule-1) and VCAM-1 (vascular cell adhesion molecule-1), through their cognate ligands [9,10]. E-selectin is expressed exclusively by ECs in rapid response to inflammatory stimuli (e.g., TNF-a and IL-1β). E-selectin recognizes various glycoprotein ligands expressed on cancer cells, including a specific sialofucosylated glycoform of CD44, PSGL1, CD24, MUC1 and LGALS3BP [11-13]. Cancer cell interaction with E-selectin seems to be the initial step for CTC extravasation and is essential for metastasis [14-16]. It has been reported that bone vascular E-selectin directly captures breast cancer cells to promote bone metastasis [17]. Consistently, atrial natriuretic peptide (ANP) prevents cancer metastasis by suppressing E-selectin expression by ECs [18]. Subsequently, ICAM-1 and VCAM-1 on ECs allow adhesion of cancer cells to ECs. ICAM-1 forms Y-shaped covalent homodimers at the cell surface

[19,20], which forcefully bind to the abnormal glycoform of MUC1 associated with cancer cells [21-24]. VCAM-1 is expressed on the luminal and lateral side of ECs in response to inflammatory factors. VCAM-1 also increases the adhesion of various subsets of leukocytes [25-27] and tumor cells [28-30] via recognition of integrins, such as VLA-4 (late activation antigen-4) or integrin a4. Pretreatment of inflammatory factors, such as TNFa, IL-1b and SDF-1, or exposure to surgical stress or sepsis [31] increased VCAM-1 expression on pulmonary ECs of mice, leading to increased numbers of lung metastatic nodules after intravenous injection of tumor cells [32-35].

E-selectin [36,37], ICAM-1 [38,39] and VCAM-1 [40,41] are NF-kB target genes in ECs. When endothelial cells receive inflammatory stimuli, such as TNFa or lipopolysaccharide (LPS), the IKK kinase complex, containing IKKa, IKKβ and NEMO (IKKg), phosphorylates IkBa and targets IkBa for proteasomal degradation. Without the IkBa suppressor, NF-kB transcriptional factors enter the nucleus and bind to specific promoters to activate transcription of downstream target genes [42,43]. Although IKKa and IKKβ have similar structures, they exhibit differential regulatory patterns [44,45]. IKKa is dispensable for IkBa degradation [46,47], but IKKa promotes processing of the p100 precursor into p52 in the noncanonical NF-kB pathway [48]. Additionally, IKKa harbors a specific nuclear localization signaling and can directly regulate NF-kB-dependent gene transcription in the nucleus. Nuclear IKKa is recruited to NF-kB binding chromatin and phosphorylates histone H3 at Ser10 to activate NF-kB target gene transcription [49,50].

HECTD3 is a HECT-type E3 ubiquitin ligase with multiple substrates and functions [51]. HECTD3 confers chemotherapy drug resistance by ubiquitinating MALT1 [52], Caspase-8 [53], and Caspase-9 [54]. Hectd3 promoted pathogenic Th17 cell generation by ubiquitinating MALT1 and STAT3 in an experimental autoimmune encephalomyelitis (EAE) mouse model [55]. Our recent study suggested that Hectd3 promotes type I interferon production and intracellular bacterial infection by increasing K63-linked polyubiquitination of TRAF3 [56]. In most situations, HECTD3 does not target its substrates for degradation because the ubiquitination chains mediated by HECTD3 are not linked through K48 or K11. Instead, HECTD3 protects MALT1 from degradation in response to chemotherapy [52]. However, the role of HECTD3 in cancer metastasis has not been previously reported.

In this study, we utilized multiple mouse models to examine the function of HECTD3 in tumor metastasis and observed that HECTD3 promotes adhesion of tumor cells to the vascular endothelium by upregulating expression of adhesion molecules on ECs in response to inflammatory conditions, which promotes tumor hematogenous metastasis. The mechanism involves HECTD3 ubiquitinates IKKa to promote its stability and nuclear kinase activity toward histone H3, eventually potentiating NF-kB-mediated gene transcription. We demonstrated that inhibition of the HECTD3-IKKa axis effectively inhibited tumor metastasis induced by systemic inflammation.

Results

Hectd3 deficiency inhibits inflammation-induced tumor metastasis in mice

As mentioned earlier, surgery may promote metastasis by increasing tumor cell dissemination and inducing systemic inflammation. To determine the role of Hectd3 in tumor metastasis, we analyzed metastasis susceptibility in Hectd3-deficient mice utilizing two malignant mouse breast cancer metastasis models after surgery. We generated PyMT-induced mouse breast tumor cells by intraductal injection of lentivirus overexpressing PyMT into the mammary duct of wild type (WT) female FVB mice [57]. Then, we transplanted PyMT-induced mouse breast tumor cells into WT and *Hectd3*$^{-/-}$ mice and examined the lungs 2 months after resection of orthotopic tumors. Compared to WT mice, Hectd3 deficiency significantly inhibited lung metastasis (Fig. 1A) and heart metastasis (Fig. 1B). 4T1-Luc2 can spontaneously metastasize to multiple organs in BALB/c mice from the breast [58–60]. We orthotopically inoculated 4T1-Luc2 cells into the fourth mammary fat pad of WT and *Hectd3*$^{-/-}$ female BALB/c mice. Eleven days later, mice were imaged using a bioluminescent IVIS system, confirming that tumor size was consistent across animals between these two groups (Fig. 1C). On day 12, tumors were surgically removed. Tumor metastasis was monitored weekly by imaging. We found that 4T1-Luc2 tumor metastasis was markedly suppressed in *Hectd3*$^{-/-}$ mice (Fig. 1C-D). In addition, Hectd3 deficiency significantly prolonged mouse survival (Fig. 1E), demonstrating that Hectd3 deficiency in the tumor microenvironment inhibits metastasis.

To further investigate whether Hectd3 deficiency inhibits the metastasis of cancer cells to inflamed organs, we intravenously injected WT and *Hectd3*$^{-/-}$ female FVB mice with LPS, which mimics systemic inflammation in response to surgical stress [6,61], followed by tail-vein injection of PyMT-induced mouse breast tumor cells. *Hectd3* knockout (KO) had no effect on lung metastasis in the absence of LPS pretreatment. However, LPS remarkably increased the number of lung metastatic nodules and the weight of the lung in both WT and *Hectd3*$^{-/-}$ mice. However, increased LPS-induced lung metastasis was significantly compromised in *Hectd3*$^{-/-}$ mice (Fig. 1F-H). Consistently, *Hectd3* KO significantly prolonged mouse survival (Fig. 1I). Similar results were observed when we used 4T1-Luc2 breast tumor cells and B16-F10 melanoma cells (Figure S1A-F). Taken together, we conclude that Hectd3 deficiency suppresses inflammation-induced metastasis.

It is well known that inflammation is one of the hallmarks of cancer [62] and that inflammation promotes metastasis [63]. Therefore, we next tested whether *Hectd3* KO inhibits metastasis of spontaneous breast tumors developed from *MMTV-Neu* transgenic mice in the FVB genetic background. We found that 76% of *MMTV-Neu;Hectd3*$^{+/+}$ mice developed lung metastases (Figure S1G). These data are in agreement with previous reports [64–66]. In contrast, only 41% of *MMTV-Neu;Hectd3*$^{-/-}$ mice developed lung metastasis (Figure S1G). Additionally, *MMTV-Neu;Hectd3*$^{-/-}$ mice exhibited far fewer tumor lesions than control mice, especially beyond 8 weeks after tumor onset (Figure S1H-I). Interestingly, mammary tumor latency between the two groups was indistinctive (Figure S1J).

HECTD3 promotes adhesion of tumor cells to human umbilical vein endothelial cells (HUVECs) by upregulating E-selectin, ICAM-1 and VCAM-1 expression in HUVECs

Adhesion of cancer cells to ECs is a key step for metastasis. Systemic inflammation provoked by surgical trauma or LPS stimulation increases the adhesion of CTCs to the vascular endothelium of distant organs by upregulating adhesion molecules in the endothelium. To investigate whether expression of adhesion molecules on the endothelium is regulated by HECTD3, we isolated and validated primary HUVECs from the neonatal umbilical cord vein [67]. When we knocked down HECTD3 in HUVECs with a siRNA pool, both protein and mRNA expression levels of adhesion molecules, including E-selectin, ICAM-1 and VCAM-1, were dramatically downregulated in response to LPS (Fig. 2A-B). Similar results were observed for TNFα and IL-1β (Figure S2A-D). As a positive control, knockdown of p65/RelA abolished the induction of adhesion molecules in response to these inflammatory factors (Figs. 2A-B & S2A-D). Knockdown of HECTD3 with two different siRNAs showed similar results (Figures S2E-F). These findings suggest that HECTD3 contributes to NF-κB signaling.

Next, we assessed whether HECTD3 promotes the adhesion of tumor cells to HUVECs using an *in vitro* adhesion assay. We treated HUVECs with LPS to induce adhesion molecule expression, added suspended GFP-labeled tumor cells to allow attachment, washed away the unattached tumor cells, and quantified tumor cells adhered to HUVECs (Fig. 2C). As expected, LPS dramatically increased attachment of GFP-labeled breast cancer cells (HCC1937-GFP, MDA-MB-231-GFP and MDA-MB-468-GFP) and leukemia cells (Jurkat-GFP) to HUVECs (Figs. 2D-E). Likewise, knockdown of HECTD3 or p65 significantly inhibited attachment of cancer cells to HUVECs (Figs. 2D-E).

Subsequently, we examined whether HECTD3 functions through its E3 ligase activity. We knocked down endogenous HECTD3 and then overexpressed siRNA-resistant HECTD3 WT or HECTD3 C823A (a catalytically inactive mutant) in HUVECs using the pCDH lentivirus overexpression system. Immunoblotting results showed that overexpression of WT HECTD3 in HUVECs remarkably increased both protein and mRNA levels of E-selectin, ICAM-1 and VCAM-1 induced by LPS (Fig. 2F-G) and TNFα (Figure S2G-H). Interestingly, overexpressing HECTD3, but not C823A, rescued the downregulation of adhesion molecules induced by knockdown of endogenous HECTD3 with siRNA (Figs. 2F-G&S2G-H). These results suggest that the E3 ligase activity of HECTD3 is essential for induction of adhesion molecule expression by inflammatory factors (Figs. 2F-G&S2G-H). Consistently, overexpression of WT HECTD3 but not HECTD3 C823A mutant in HUVECs significantly increased the adhesion of cancer cells to LPS-treated HUVECs (Figures S2I-J). Finally, we inhibited expression of E-selectin, ICAM-1 and VCAM-1 using a siRNA mixture of siE-selectin, siICAM-1 and siVCAM-1, which blocked upregulation of expression of these adhesion molecules (Figure S2K), as well as the increase in tumor cell adhesion (Figs. 2H-I) induced by HECTD3 overexpression in HUVECs. These results suggest that HECTD3 promotes the adhesion of tumor cells to HUVECs by upregulating E-selectin, ICAM-1 and VCAM-1 expression in HUVECs through its E3 ligase activity.

HECTD3 increases the transcription of adhesion molecules by stabilizing IKKα and recruiting nuclear IKKα to adhesion molecule gene promoters

NF-κB is a known signaling pathway responsible for *E-selectin*, *ICAM-1* and *VCAM-1* gene transcriptional upregulation in the endothelium in response to inflammatory stimuli [36–41]. Although LPS, TNFα and IL-1β activate the NF-κB pathway through different receptors and adaptors, the extracellular signals converge on recruitment and activation of the IKK complex, which contains IKKα, IKKβ and IKKγ (NEMO). We suspected that HECTD3 regulates a key common component of the NF-κB pathway. We first knocked down HECTD3 in HUVECs, stimulated cells with LPS, TNFα, and IL-1β, and examined expression of the IKK complex and activation of the NF-κB signaling pathway. We found that protein levels of total IKKα, but not IKKβ or NEMO, decreased significantly (Figs. 3A&S3A-B). Interestingly, the changes in p-IKKα/β, p-IκBα, and total IκBα were only slightly inhibited by HECTD3 knockdown. Thus, we subsequently focused on IKKα.

We first investigated whether IKKα is essential for inducing the expression of adhesion molecules by inflammatory factors. When we knocked down IKKα, mRNA and protein expression levels of E-selectin, ICAM-1 and VCAM-1 induced by the inflammatory factors LPS (Figs. 3B-C) and TNFα (Figures S3C-D) in HUVECs were significantly decreased. Furthermore, knockdown of IKKα abolished HECTD3 overexpression-induced increases in adhesion molecule expression in HUVECs in response to LPS (Fig. 3D) and TNFα (Figure S3E). These results indicate that HECTD3 functions through IKKα.

Since HECTD3 knockdown decreased total IKKα protein levels but did not affect IκBα phosphorylation or degradation in response to inflammation (Figs. 3A & S3A-B), we hypothesized that HECTD3 promotes adhesion molecule gene transcription independent of the IKK complex [68–71]. IKKα translocates into the nucleus and phosphorylates histone H3 at Ser10 to facilitate NF-κB-dependent transcription [49,50] and is crucial for p65 binding to the ICAM-1 promoter [71]. Indeed, we demonstrated that HECTD3 knockdown dramatically decreased IKKα-mediated phosphorylation of histone H3 at Ser10 (p-H3(Ser10)), while HECTD3 overexpression increased p-H3(Ser10) (Fig. 3E). Consistently, we demonstrated that HECTD3 knockdown obviously decreased nuclear localization of IKKα in HUVECs stimulated with LPS by immunoblotting (Figure S3F) and immunofluorescence staining (Figure S3G). To determine whether IKKα was recruited to *E-selectin*, *ICAM-1* and *VCAM-1* gene promoters to increase transcription through epigenetic modifications, chromatin immunoprecipitation (ChIP) assays were performed using the IKKα antibody. As anticipated, recruitment of IKKα to these loci was obviously increased in response to LPS, while HECTD3 knockdown significantly inhibited this process (Figs. 3F-G). These results indicate that HECTD3 promotes IKKα stabilization, nuclear localization, and specific recruitment in HUVECs in response to inflammatory stimuli.

To characterize the mechanism by which HECTD3 stabilizes IKKα, we first examined *IKKα* mRNA levels after HECTD3 knockdown. There were no significant changes in *IKKα* mRNA levels (Figure S3H), implicating that the regulation may occur at the posttranscriptional level. Then, we used cycloheximide (CHX) to block protein synthesis and found that IKKα had a long half-life and that knockdown of HECTD3 promoted the degradation of IKKα (Figs. 3H-I). Next, we investigated the protein degradation pathway of IKKα by treating HECTD3 knockdown cells with the proteasome inhibitor MG132 or lysosome inhibitors

NH_4Cl and HCQS (hydroxychloroquine sulfate). As shown in Fig. 3J, both lysosome inhibitors, but not proteasome inhibitor, restored protein expression downregulation of IKKα induced by HECTD3 knockdown. These findings suggest that HECTD3 prevents IKKα from being degraded by lysosomes.

Hectd3 Interacts With Ikkα

To test whether IKKα is a HECTD3 substrate, we first tested protein interaction between these two factors. We performed coimmunoprecipitation (co-IP) experiments and demonstrated that Flag-HECTD3 immunoprecipitated exogenous IKKα and Flag-IKKα immunoprecipitated exogenous HECTD3 in HEK293T cells (Fig. 4A). Next, we demonstrated that Flag-HECTD3 immunoprecipitated the endogenous IKKα protein in HUVECs (Fig. 4B). More importantly, endogenous IKKα and HECTD3 proteins also interact with each other, as shown using an anti-IKKα antibody in normal HUVECs (Fig. 4C). Consistently, IKKα colocalized with HECTD3 in HUVECs (Fig. 4D). The interaction was not increased by inflammatory factor stimulation (Figure S4A). Furthermore, we mapped the interaction domains of HECTD3 and IKKα. Our previous studies showed that the HECTD3 DOC domain (amino acids 216–393) is responsible for recruiting substrates, including MALT1 and Caspase-8 [52,53]. We transfected several GST-fused HECTD3 truncated mutants with Flag-IKKα in HEK293T cells and performed GST pulldown assays with glutathione sepharose beads. We found that the DOC domain also mediates the interaction between HECTD3 and IKKα (Fig. 4E). Similarly, we constructed a series of IKKα truncated mutants fused with GST and transfected them with Flag-HECTD3 in HEK293T cells, performing a GST pulldown experiment. We demonstrated that IKKα interacted with HECTD3 through its SDD domain (amino acids 408–665) (Figs. 4F&S4B).

HECTD3 ubiquitinates IKKα with K27- and K63-linked polyubiquitin chains at K296 and increases IKKα protein stability and kinase activity

Next, we investigated whether HECTD3 ubiquitinates IKKα. As expected, HECTD3, but not the HECTD3 C823A inactive mutant, significantly increased polyubiquitination of IKKα in HEK293T cells (Fig. 5A). Additionally, we showed that knockdown of HECTD3 decreased endogenous IKKα polyubiquitination in HUVECs (Fig. 5B). Moreover, we performed an *in vitro* ubiquitination assay using purified components, including E1, E2 (UbcH5b), E3 (HECTD3 or HECTD3 C823A) (Fig. 5C), Flag-IKKα, HA-Ub, and ATP. As shown in Fig. 5D, HECTD3 dramatically increased Flag-IKKα polyubiquitination in an E3 ligase activity-dependent manner.

The IKKα protein contains 51 lysine (K) residues. To identify the K residues responsible for HECTD3-mediated polyubiquitination, we artificially divided IKKα into 9 regions and constructed a series of mutants termed IKKα R1-9 in which we replaced all K residues with arginine (R) residues. We found that HECTD3 induced polyubiquitination of IKKα (WT) and its mutants, with the exception of IKKα R4 (Figure S5A). These results implied that region 4 of IKKα, which contains K296, K311, and K322, contains potential ubiquitination sites. We further identified K296 as a unique ubiquitination site because HECTD3 could not increase polyubiquitination of IKKα K296R (Fig. 5E). Likewise, K296R mutation did not affect

the protein-protein interaction between HECTD3 and IKKα (Figure S5B). Taken together, these findings suggest that HECTD3 catalyzes the polyubiquitination of IKKα at K296.

Next, we determined the linkage of IKKα polyubiquitination mediated by HECTD3. Using a series of Ub mutants (K only), we found that K27- and K63-only Ub supported HECTD3-catalyzed IKKα polyubiquitination, similar to WT Ub (Figs. 5F&S5C). We further confirmed this result using linkage-specific anti-Ub antibodies. HECTD3-mediated IKKα polyubiquitination was recognized by specific antibodies against K27-polyUb and K63-polyUb but not K48-poly Ub (Fig. 5G). Consistently, knockdown of endogenous HECTD3 specifically decreased both K27-linked and K63-linked, but not K48-linked, polyubiquitination of IKKα in HEK293T cells (Figure S5D). These findings suggest that HECTD3 ubiquitinates IKKα with a mixture of K27-linked and K63-linked polyubiquitin chains.

To test the consequence of IKKα ubiquitination by HECTD3, we first compared the IKKα protein stabilities of K296R and WT in HEK293T cells. Compared to WT, K296R exhibited a shorter protein half-life, as measured by CHX chase experiments (Fig. 5H). Unlike WT IKKα, K296R failed to promote expression of E-selectin, ICAM-1 and VCAM-1 in response to TNFα (Figure S5E). Additionally, overexpression of WT IKKα rescued HECTD3 knockdown-induced downregulation of adhesion molecule expression in HUVECs under TNFα stimulation, but K296R failed to do so (Figure S5E). To eliminate the impact of endogenous IKKα, we generated *IKKα* KO HUVECs using CRISPR/Cas9 technology. IKKα depletion dramatically inhibited but did not abolish the expression levels of p-H3(Ser10) and E-selectin, ICAM-1 and VCAM-1 in response to LPS and TNFα stimulation (Figs. 5I&S5F). As expected, WT IKKα, but not IKKα K296R, overexpression in *IKKα* KO HUVECs rescued the expression levels of p-H3 (Ser10) and the three adhesion molecules (Figs. 5I&S5F).

To test whether HECTD3-mediated IKKα ubiquitination promotes IKKα nuclear translocation, we compared the subcellular distribution of IKKα and IKKα K296R in HUVECs by collecting cytoplasmic and nuclear protein fractions for immunoblotting. K296R presented a subcellular distribution similar to that of WT (Figure S5G). We speculate that the interaction between HECTD3 and IKKα is sufficient to keep IKKα in the nucleus. Alternatively, HECTD3 may increase IKKα nuclear localization by stabilizing IKKα. Nevertheless, polyubiquitination of IKKα induced by HECTD3 does not regulate the subcellular localization of IKKα.

Taken together, these results reveal that IKKα is a kinase for histone H3 and other substrates, and it is reasonable to deduce that HECTD3-mediated IKKα ubiquitination may promote its kinase activity. We next performed *in vitro* kinase assays to measure the kinase activities of IKKα WT, K296R, and S176/180A proteins purified from HEK293T cells. IKKα S176/180A is a well-known kinase dead mutant [72]. Given that IKKα phosphorylates histone H3 at Ser10 [49,50] and IκBα at Ser32 and Ser36 [73], we purified GST-fused histone H3 and IκBα from *E. coli* as substrates of IKKα. Notably, WT IKKα robustly phosphorylated GST-H3, while IKKα K296R and IKKα S176/180A showed only weak kinase activities toward GST-H3 (Fig. 5J). Consistently, knockdown of endogenous HECTD3 in HEK293T cells decreased the kinase activity of IKKα (Fig. 5K), and overexpression of HECTD3, but not HECTD3 C823A, in HEK293T

cells significantly increased the kinase activity of WT IKKα but not IKKα-K296R (Fig. 5L). Furthermore, similar results were obtained using GST-IκBα as the substrate in the kinase assay (Figures S5H-I). These results suggest that IKKα ubiquitination mediated by HECTD3 promotes IKKα kinase activity independent of IKKα protein stability.

Dimerization is necessary for IKKα activation [48,74,75]. Therefore, we tested whether HECTD3-mediated IKKα ubiquitination promotes its dimerization using co-IP experiments in HEK293T cells cotransfected with GST-IKKα and Flag-IKKα (WT, K296R, S176/180A) or IKKβ. We found that the K296R mutation did not affect dimerization of IKKα (Figure S5J). Interestingly, we found that purified GST-H3, but not GST-IκBα, pulled down more Flag-IKKα than Flag-IKKα K296R in HEK293T cell lysates (Fig. 5M&S5K). Therefore, it is plausible that HECTD3-mediated IKKα ubiquitination increases the interaction between IKKα and histone H3 so that IKKα can efficiently phosphorylate it. However, this mechanism did not hold up for IκBα.

Hectd3 promotes adhesion of tumor cells to mouse lung vascular endothelial cells through IKKα under inflammatory conditions

To investigate whether Hectd3 functions similarly in mouse vascular endothelial cells, we purified and cultured mouse pulmonary vascular endothelial cells (mECs) using Dynabeads coated with anti-CD31 antibody. *Hectd3* KO inhibited the induction of E-selectin, Icam-1 and Vcam-1 in mECs in response to LPS and TNFα stimuli, as examined by qRT-PCR (Figs. 6A&S6A) and immunoblotting (Figs. 6B&S6B). Consistently, *Hectd3* KO decreased the protein levels of IKKα and p-H3 (Ser10) in mECs (Figs. 6B&S6B). These results suggest that Hectd3 activates IKKα and promotes adhesion molecule expression in mECs under inflammatory stimulation.

As shown at the beginning of this study, *Hectd3*$^{-/-}$ mice exhibited significantly decreased lung metastasis when tumor cells were injected through the tail vein and mice were treated with LPS in advance. We next examined whether Hectd3 deficiency suppresses tumor metastasis by inhibiting adhesion molecule expression to inhibit tumor cell colonization in the lung. To address this question, we conducted *in vivo* adhesion assays (Fig. 6C) by injecting GFP-labeled PyMT-induced mouse breast tumor cells into WT or *Hectd3*$^{-/-}$ mice through the tail vein. Mice were treated with LPS stimulation for 5 h before tumor cell injection and sacrificed and perfused with PBS 20 h after tumor cell injection. Immunofluorescence was performed to detect GFP-positive tumor cells in the lung. As a result, increased tumor cells infiltrated into WT mouse lung tissues than into *Hectd3*$^{-/-}$ mouse lung tissues (Fig. 6D). We confirmed this result by digesting the lung tissues of WT and *Hectd3*$^{-/-}$ mice and performing flow cytometry analyses (Fig. 6E). Immunoblotting and qRT-PCR analysis of GFP protein and mRNA expression in mouse lung tissues further validated this conclusion (Figure S6C-D). Taken together, these data suggest that Hectd3 depletion decreases lung colonization of tumor cells under inflammatory conditions.

To further confirm that Hectd3 promotes tumor metastasis specifically through endothelial cells, we created *Hectd3* conditional knockin (KI) mice in endothelial cells *in vivo*. We generated loxP-Stop-loxP-*Hectd3*^{KI}-GFP C57BL/6 strain mice by inserting the targeting sequence of CAG pr-loxP-Stop-loxP-*Hectd3* CDS-P2A-eGFP-WPRE-pA into the Rosa26 site using the EGE system based on CRISPR/Cas9 developed by Beijing Biocytogen Co., Ltd. We crossed our loxP-Stop-loxP-*Hectd3*^{KI}-GFP mice with a background of Cre recombinase expression driven by the Tie2 promoter, which allows specific deletion of the Stop sequence to overexpress Hectd3 and GFP in the endothelium (Fig. 6F). We isolated pulmonary vascular endothelial cells from *Tie2-Cre*$^{+}$;*Hectd3*^{KI} and *Tie2-Cre*$^{-}$;*Hectd3*^{KI} mice and assessed the expression of Hectd3 and GFP. As expected, Hectd3 and GFP protein expression levels were robustly increased in mECs from *Tie2-Cre*$^{+}$;*Hectd3*^{KI} mice (Fig. 6G). Importantly, IKKα protein levels were also increased in the endothelium of *Tie2-Cre*$^{+}$;*Hectd3*^{KI} mice (Fig. 6G). Subsequently, we treated mice with LPS for 5 h and injected B16-F10 melanoma cells into the tail vein. Twenty days later, *Tie2-Cre*$^{+}$;*Hectd3*^{KI} mice presented significantly increased pulmonary metastasis compared to *Tie2-Cre*$^{-}$;*Hectd3*^{KI} control mice (Figs. 6H-J). Furthermore, similar results were obtained using whole body *Hectd3*^{KI} mice by crossing CMV-Cre mice with our loxP-Stop-loxP-*Hectd3*^{KI}-GFP mice (Figure S6E-F). These animal experimental data confirm that Hectd3 promotes tumor metastasis by enhancing tumor cell colonization mediated by vascular endothelial cells in response to inflammation.

Ikkα Kinase Inhibitor Bay32-5915 Suppresses Tumor Lung Metastasis

HECTD3 promotes adhesion molecule expression by ubiquitinating IKKα, and *Hectd3* KO inhibits tumor metastasis. Currently, there are no effective HECTD3 inhibitors available, so we examined whether an IKKα inhibitor could suppress tumor metastasis. The small molecule 8-hydroxyquinoline-2-carboxylic acid (BAY 32-5915) is a reported IKKα-specific kinase inhibitor [76]. We demonstrated that BAY 32-5915 significantly inhibited induction of p-H3 (Ser10) and adhesion molecules in HUVECs in response to LPS and TNFα (Fig. 7A). To our surprise, levels of p-IKKα/β and p-p65 in HUVECs treated with BAY 32-5915 were significantly increased over time under stimulation of LPS and TNFα, while there were no significant changes in the phosphorylation or degradation of IκBα (Figure S7A-B). This was likely caused by a negative feedback mechanism of IKKα inhibition by BAY 32-5915, which somehow activated a compensatory pathway. Next, we pretreated HUVECs with different concentrations of BAY 32-5915 for 12 h and then added either LPS or TNFα for 4 h. BAY 11-7082, a classic inhibitor of the NF-κB pathway, was used as a positive control. Results showed that BAY 32-5915 inhibited expression of p-H3(Ser10), E-selectin, ICAM-1, and VCAM-1 in HUVECs in a concentration-dependent manner (Fig. 7A).

To test whether BAY 32-5915 could inhibit tumor metastasis *in vivo*, we pretreated BALB/c mice with BAY 32-5915 (25 mg/kg) or BAY 11-7082 by intravenous injection for 24 h, injected LPS (1 mg/kg) intravenously for 5 h, and then injected 4T1-Luc2 breast tumor cells through the tail vein. Compared to the vehicle control, BAY 32-5915 and BAY 11-7082 significantly reduced the number of pulmonary metastatic nodules (Fig. 7B). We confirmed this result using another metastasis model. PyMT-induced breast tumor cells were injected by tail vein into FVB mice that were pretreated with vehicle or BAY 32-

5915 (12.5 or 25 mg/kg) for 24 h and LPS (1 mg/kg) for 5 h by intravenous injection. The number of pulmonary metastatic nodules and the lung weight gradually decreased with increasing BAY 32-5915 concentrations (Fig. 7C-E). These results indicate that the IKKα kinase inhibitor BAY 32-5915 suppresses tumor lung metastasis induced by inflammation.

Discussion

Cancer metastasis is a multistep process by which tumor cells disseminate from their primary site, circulate in the vessels, and eventually form secondary tumors at a distant site [77]. Most CTCs expire in the bloodstream due to shear stress and attack of the immune system, but a small proportion of tumor cells infiltrate distant organs and survive. Surgery, including biopsy, is a double-edged sword that removes the primary tumor but induces tumor-dormancy escape and subsequent metastatic outgrowth by impairing tumor-specific immunity [60,78–80] or by producing a transient immunosuppressive state associated with wound healing [81–83]. In other words, surgery triggers abundant detachment of tumor cells readily drilling into the vasculature [3,4] and induces systemic inflammation that assists adhesion of tumor cells to distant ECs [5,6,84]. A retrospective study examining the incidence of cancer recurrence in patients with lung cancer surgery showed that perioperative treatment with ANP, which inhibits the expression of E-selectin on ECs, improved relapse-free survival after surgery compared to surgery alone [18]. Another retrospective analysis of tumor recurrence in patients undergoing breast cancer surgery revealed that preoperative treatment with ketorolac was related to a significant decrease in recurrence and mortality after surgery [85]. Surprisingly, preoperative stimulation with ketoralac and resolvins (RvD2, RvD3, or RvD4) for resolution of inflammation dramatically reduced lung metastasis aroused by primary tumor removal in multiple mouse models [60]. Surgery also increases the recruitment of myeloid-derived suppressor cells (MDSCs) into the lung to form premetastatic niches, and blockade of this recruitment with 5-azacytidine and entinostat effectively inhibits lung metastasis in a mouse model [86] Therefore, it is important to identify additional therapeutic targets and drugs to prevent cancer metastasis caused by inflammation.

In this study, we provided evidence to support the notion that HECTD3 promotes tumor cell adhesion to ECs and metastasis by ubiquitinating IKKα in response to inflammation. First, we demonstrated that *Hectd3* KO inhibited distant tumor relapse in spontaneous metastasis models in response to surgery or systemic inflammation. Second, HECTD3 depletion in HUVECs and mouse ECs blocked inflammation-induced adhesion molecule expression and tumor cell adhesion to ECs *in vitro* and *in vivo*. In addition, Hectd3 overexpression specifically in mECs increased tumor metastasis *in vivo*. Moreover, we characterized the molecular mechanism by which HECTD3 promotes metastasis. HECTD3 ubiquitinates IKKα with K63- and K27-linked polyubiquitin chains at K296, which prevents IKKα degradation by lysosomes and increases nuclear IKKα kinase activity. Activated IKKα is recruited to the promoters of adhesion molecules and phosphorylates histone H3 at Ser10 to facilitate transcription. Finally, we showed that an IKKα kinase inhibitor significantly suppressed inflammation-induced adhesion molecule

expression and cancer metastasis *in vivo*. Taken together, the HECTD3-IKKα axis may serve as an effective prevention target for inflammation-induced cancer metastasis (Fig. 7F).

It has long been recognized that metastasis can be enhanced by acute or chronic inflammation, such as in response to IL-1β or LPS, which induces endothelial adhesion molecules that facilitate adhesion of cancer cells to ECs. Adhesion molecules, such as E-selectin, ICAM-1 and VCAM-1, have fundamental functions in leukocytes and hemostasis by mediating the rolling of leukocytes on activated ECs and transmigration through endothelial cell junctions. Unfortunately, tumor cells can utilize the same route to achieve distant metastasis, especially when the vascular endothelium undergoes inflammatory stimulation, such as in response to surgery. In the bloodstream, CTCs also aberrantly express adhesion molecules to interact with platelets and immune cells, such as neutrophils, monocytes, and macrophages, as well as endothelial cells [6,87–91]. This provides a potential approach to suppress metastasis by interrupting adhesive interactions. *E-selectin*$^{-/-}$ mice show bone metastasis blockade [17]. Ang2 (angiopoietin-2) increases ICAM-1 expression in ECs so that anti-Ang2 therapy limits the outgrowth of micrometastases [59]. The anti-integrin α4 mAb Natalizumab reduced melanoma pulmonary metastasis [92]. Anti-VCAM-1 or anti-integrin α4 mAbs also dramatically reduced bone metastasis in breast cancer [30]. Here, we showed that HECTD3 and IKKα control inflammatory adhesion molecule expression and that inhibition of HECTD3 genetically or IKKα pharmacologically suppresses metastasis. It is warranted to develop small molecule inhibitors for HECTD3 and IKKα for tumor metastasis prevention, especially in patients who undergo surgical removal of the primary tumor.

IKKα is dispensable for IκBα phosphorylation and degradation but remains essential for NF-κB-dependent transcription because of its nuclear kinase activity. In the nucleus, IKKα is recruited to the NF-κB transcription complex to phosphorylate multiple substrates, such as histone H3 at Ser10 [49,50], CBP at Ser1382/1386 [69], p65 at Ser536 [93], and SMRT at Ser2410 [94], to promote NF-κB-dependent gene transcription. A recent research showed that IKKα phosphorylated histone H3.3 at Ser31 to amplify stimulation-induced transcription[95]. Although we only demonstrated histone H3 as a substrate of IKKα in this study, we cannot exclude the possibility that IKKα phosphorylates other substrates. Additionally, nuclear IKKα has been shown to regulate the DNA damage response, radioresistance, apoptosis, and the cell cycle [96–99]. Whether HECTD3 regulates other functions of IKKα remains to be investigated.

Although it has been reported that IKKα ubiquitination promotes its nuclear translocation in hepatoma cells [68], its E3 ligase and modification details have not been fully elucidated. For the first time, we identified HECTD3 as an IKKα E3 ligase that promotes K63- and K27-linked polyubiquitination at K296. Ubiquitination promotes IKKα protein stability and kinase activity. Although it remains unknown how the K63- and K27-linked polyubiquitination of IKKα affects its protein stability, lysosome-dependent degradation may be involved since lysosome inhibitors restored protein levels of IKKα after knockdown of HECTD3 (Fig. 3J). Furthermore, we found that blocking ubiquitination of IKKα inhibited the interaction of IKKα with the target protein histone H3 but not IκBα. However, how ubiquitination promotes the kinase activity of IKKα needs further investigation.

In summary, our data characterize the function of the HECTD3-IKKα axis in the adhesion of tumor cells to the endothelium through the NF-κB signaling pathway, which provides a potential strategy for tumor hematogenous metastasis prevention and treatment.

Declarations

Acknowledgments

We thank D. Ai and C. H. Zhang (School of Basic Medical Science, Tianjin Medical University, Tianjin) for Tie2-Cre mice and Y. G. Tao (Institute of Medical Sciences, Xiangya Hospital, Central South University, Changsha) for IKKa plasmids.

This work was supported by grants from the National Postdoctoral Program for Innovative Talents (BX20190088), the China Postdoctoral Science Foundation (2019 M662869), the National Key Research and Development Program of China (2018YFC2000400 to C. Chen), the Shenzhen Municipal Government of China (KQTD20170810160226082), the National Natural Science Foundation of China (81773149 to Y. Kong; 81830087, U1602221, and 31771516 to C. Chen; 81672639 to Z. Zhou; 81802671 and 81872414 to D. Jiang; 81772847 to R. Liu), the Project of Innovative Research Team of Yunnan Province (2019HC005) and the Yunnan Applied Basic Research Projects (2018FB134 to Y. Kong).

Author contributions

F. Li performed most experiments with crucial help from H.L., H.Y., J.X., H.X., X.C., M.H., Z.C., C.Y., W.L., H.Z., L.Z., Y.W., F.G., Z.L., W.Z., Z.Z., R.L., D.J., N.X., Y.K. and F.L. C.C. wrote the manuscript and conceived and designed the study. All authors discussed the results and commented on the manuscript.

References

1 Mehlen, P. & Puisieux, A. Metastasis: a question of life or death. *Nature reviews. Cancer* **6**, 449-458, doi:10.1038/nrc1886 (2006).

2 Braun, S. *et al.* A pooled analysis of bone marrow micrometastasis in breast cancer. *The New England journal of medicine* **353**, 793-802, doi:10.1056/NEJMoa050434 (2005).

3 Koch, M. *et al.* Detection of hematogenous tumor cell dissemination predicts tumor relapse in patients undergoing surgical resection of colorectal liver metastases. *Annals of surgery* **241**, 199-205, doi:10.1097/01.sla.0000151795.15068.27 (2005).

4 Funaki, S. *et al.* Novel approach for detection of isolated tumor cells in pulmonary vein using negative selection method: morphological classification and clinical implications. *European journal of cardio-thoracic surgery : official journal of the European Association for Cardio-thoracic Surgery* **40**, 322-327, doi:10.1016/j.ejcts.2010.11.029 (2011).

5 Giavazzi, R., Foppolo, M., Dossi, R. & Remuzzi, A. Rolling and adhesion of human tumor cells on vascular endothelium under physiological flow conditions. *The Journal of clinical investigation* **92**, 3038-3044, doi:10.1172/JCI116928 (1993).

6 McDonald, B. *et al.* Systemic inflammation increases cancer cell adhesion to hepatic sinusoids by neutrophil mediated mechanisms. *International journal of cancer* **125**, 1298-1305, doi:10.1002/ijc.24409 (2009).

7 Kienast, Y. *et al.* Real-time imaging reveals the single steps of brain metastasis formation. *Nature medicine* **16**, 116-122, doi:10.1038/nm.2072 (2010).

8 Stoletov, K. *et al.* Visualizing extravasation dynamics of metastatic tumor cells. *Journal of cell science* **123**, 2332-2341, doi:10.1242/jcs.069443 (2010).

9 Reymond, N., d'Agua, B. B. & Ridley, A. J. Crossing the endothelial barrier during metastasis. *Nature reviews. Cancer* **13**, 858-870, doi:10.1038/nrc3628 (2013).

10 Lafrenie, R. M., Buchanan, M. R. & Orr, F. W. Adhesion molecules and their role in cancer metastasis. *Cell biophysics* **23**, 3-89, doi:10.1007/BF02796507 (1993).

11 Miles, F. L., Pruitt, F. L., van Golen, K. L. & Cooper, C. R. Stepping out of the flow: capillary extravasation in cancer metastasis. *Clinical & experimental metastasis* **25**, 305-324, doi:10.1007/s10585-007-9098-2 (2008).

12 Strell, C. & Entschladen, F. Extravasation of leukocytes in comparison to tumor cells. *Cell communication and signaling : CCS* **6**, 10, doi:10.1186/1478-811X-6-10 (2008).

13 Shirure, V. S., Reynolds, N. M. & Burdick, M. M. Mac-2 binding protein is a novel E-selectin ligand expressed by breast cancer cells. *PloS one* **7**, e44529, doi:10.1371/journal.pone.0044529 (2012).

14 Laubli, H. & Borsig, L. Selectins promote tumor metastasis. *Seminars in cancer biology* **20**, 169-177, doi:10.1016/j.semcancer.2010.04.005 (2010).

15 St Hill, C. A. Interactions between endothelial selectins and cancer cells regulate metastasis. *Frontiers in bioscience* **16**, 3233-3251, doi:10.2741/3909 (2011).

16 Barthel, S. R. *et al.* Definition of molecular determinants of prostate cancer cell bone extravasation. *Cancer research* **73**, 942-952, doi:10.1158/0008-5472.CAN-12-3264 (2013).

17 Esposito, M. *et al.* Bone vascular niche E-selectin induces mesenchymal-epithelial transition and Wnt activation in cancer cells to promote bone metastasis. *Nature cell biology* **21**, 627-639, doi:10.1038/s41556-019-0309-2 (2019).

18 Nojiri, T. *et al.* Atrial natriuretic peptide prevents cancer metastasis through vascular endothelial cells. *Proceedings of the National Academy of Sciences of the United States of America* **112**, 4086-4091, doi:10.1073/pnas.1417273112 (2015).

19 Miller, J. *et al.* Intercellular adhesion molecule-1 dimerization and its consequences for adhesion mediated by lymphocyte function associated-1. *The Journal of experimental medicine* **182**, 1231-1241, doi:10.1084/jem.182.5.1231 (1995).

20 Yang, Y. *et al.* Structural basis for dimerization of ICAM-1 on the cell surface. *Molecular cell* **14**, 269-276, doi:10.1016/s1097-2765(04)00204-7 (2004).

21 Gendler, S. J. MUC1, the renaissance molecule. *Journal of mammary gland biology and neoplasia* **6**, 339-353, doi:10.1023/a:1011379725811 (2001).

22 Regimbald, L. H. *et al.* The breast mucin MUCI as a novel adhesion ligand for endothelial intercellular adhesion molecule 1 in breast cancer. *Cancer research* **56**, 4244-4249 (1996).

23 Hayashi, T. *et al.* MUC1 mucin core protein binds to the domain 1 of ICAM-1. *Digestion* **63 Suppl 1**, 87-92, doi:10.1159/000051917 (2001).

24 Rahn, J. J. *et al.* MUC1 mediates transendothelial migration in vitro by ligating endothelial cell ICAM-1. *Clinical & experimental metastasis* **22**, 475-483, doi:10.1007/s10585-005-3098-x (2005).

25 Wittchen, E. S. Endothelial signaling in paracellular and transcellular leukocyte transmigration. *Frontiers in bioscience* **14**, 2522-2545, doi:10.2741/3395 (2009).

26 Ley, K., Laudanna, C., Cybulsky, M. I. & Nourshargh, S. Getting to the site of inflammation: the leukocyte adhesion cascade updated. *Nature reviews. Immunology* **7**, 678-689, doi:10.1038/nri2156 (2007).

27 Freedman, A. S. *et al.* Adhesion of human B cells to germinal centers in vitro involves VLA-4 and INCAM-110. *Science* **249**, 1030-1033, doi:10.1126/science.1697696 (1990).

28 Taichman, D. B. *et al.* Tumor cell surface alpha 4 beta 1 integrin mediates adhesion to vascular endothelium: demonstration of an interaction with the N-terminal domains of INCAM-110/VCAM-1. *Cell regulation* **2**, 347-355, doi:10.1091/mbc.2.5.347 (1991).

29 Juneja, H. S., Schmalsteig, F. C., Lee, S. & Chen, J. Vascular cell adhesion molecule-1 and VLA-4 are obligatory adhesion proteins in the heterotypic adherence between human leukemia/lymphoma cells and marrow stromal cells. *Experimental hematology* **21**, 444-450 (1993).

30 Lu, X. *et al.* VCAM-1 promotes osteolytic expansion of indolent bone micrometastasis of breast cancer by engaging alpha4beta1-positive osteoclast progenitors. *Cancer cell* **20**, 701-714, doi:10.1016/j.ccr.2011.11.002 (2011).

31 Rice, G. E. & Bevilacqua, M. P. An inducible endothelial cell surface glycoprotein mediates melanoma adhesion. *Science* **246**, 1303-1306, doi:10.1126/science.2588007 (1989).

32 Garofalo, A. *et al.* Involvement of the very late antigen 4 integrin on melanoma in interleukin 1-augmented experimental metastases. *Cancer research* **55**, 414-419 (1995).

33 Okahara, H., Yagita, H., Miyake, K. & Okumura, K. Involvement of very late activation antigen 4 (VLA-4) and vascular cell adhesion molecule 1 (VCAM-1) in tumor necrosis factor alpha enhancement of experimental metastasis. *Cancer research* **54**, 3233-3236 (1994).

34 Cardones, A. R., Murakami, T. & Hwang, S. T. CXCR4 enhances adhesion of B16 tumor cells to endothelial cells in vitro and in vivo via beta(1) integrin. *Cancer research* **63**, 6751-6757 (2003).

35 Higashiyama, A., Watanabe, H., Okumura, K. & Yagita, H. Involvement of tumor necrosis factor alpha and very late activation antigen 4/vascular cell adhesion molecule 1 interaction in surgical-stress-enhanced experimental metastasis. *Cancer immunology, immunotherapy : CII* **42**, 231-236, doi:10.1007/s002620050275 (1996).

36 Kaszubska, W. *et al.* Cyclic AMP-independent ATF family members interact with NF-kappa B and function in the activation of the E-selectin promoter in response to cytokines. *Molecular and cellular biology* **13**, 7180-7190, doi:10.1128/mcb.13.11.7180 (1993).

37 Lewis, H., Kaszubska, W., DeLamarter, J. F. & Whelan, J. Cooperativity between two NF-kappa B complexes, mediated by high-mobility-group protein I(Y), is essential for cytokine-induced expression of the E-selectin promoter. *Molecular and cellular biology* **14**, 5701-5709, doi:10.1128/mcb.14.9.5701 (1994).

38 Hou, J., Baichwal, V. & Cao, Z. Regulatory elements and transcription factors controlling basal and cytokine-induced expression of the gene encoding intercellular adhesion molecule 1. *Proceedings of the National Academy of Sciences of the United States of America* **91**, 11641-11645, doi:10.1073/pnas.91.24.11641 (1994).

39 Roebuck, K. A., Rahman, A., Lakshminarayanan, V., Janakidevi, K. & Malik, A. B. H2O2 and tumor necrosis factor-alpha activate intercellular adhesion molecule 1 (ICAM-1) gene transcription through distinct cis-regulatory elements within the ICAM-1 promoter. *The Journal of biological chemistry* **270**, 18966-18974, doi:10.1074/jbc.270.32.18966 (1995).

40 Neish, A. S., Williams, A. J., Palmer, H. J., Whitley, M. Z. & Collins, T. Functional analysis of the human vascular cell adhesion molecule 1 promoter. *The Journal of experimental medicine* **176**, 1583-1593, doi:10.1084/jem.176.6.1583 (1992).

41 Iademarco, M. F., McQuillan, J. J., Rosen, G. D. & Dean, D. C. Characterization of the promoter for vascular cell adhesion molecule-1 (VCAM-1). *The Journal of biological chemistry* **267**, 16323-16329

(1992).

42 Gilmore, T. D. Introduction to NF-kappaB: players, pathways, perspectives. *Oncogene* **25**, 6680-6684, doi:10.1038/sj.onc.1209954 (2006).

43 Solt, L. A. & May, M. J. The IkappaB kinase complex: master regulator of NF-kappaB signaling. *Immunologic research* **42**, 3-18, doi:10.1007/s12026-008-8025-1 (2008).

44 Tanaka, M. *et al.* Embryonic lethality, liver degeneration, and impaired NF-kappa B activation in IKK-beta-deficient mice. *Immunity* **10**, 421-429, doi:10.1016/s1074-7613(00)80042-4 (1999).

45 Sil, A. K., Maeda, S., Sano, Y., Roop, D. R. & Karin, M. IkappaB kinase-alpha acts in the epidermis to control skeletal and craniofacial morphogenesis. *Nature* **428**, 660-664, doi:10.1038/nature02421 (2004).

46 Chu, W. M. *et al.* JNK2 and IKKbeta are required for activating the innate response to viral infection. *Immunity* **11**, 721-731, doi:10.1016/s1074-7613(00)80146-6 (1999).

47 Hu, Y. *et al.* Abnormal morphogenesis but intact IKK activation in mice lacking the IKKalpha subunit of IkappaB kinase. *Science* **284**, 316-320, doi:10.1126/science.284.5412.316 (1999).

48 Senftleben, U. *et al.* Activation by IKKalpha of a second, evolutionary conserved, NF-kappa B signaling pathway. *Science* **293**, 1495-1499, doi:10.1126/science.1062677 (2001).

49 Yamamoto, Y., Verma, U. N., Prajapati, S., Kwak, Y. T. & Gaynor, R. B. Histone H3 phosphorylation by IKK-alpha is critical for cytokine-induced gene expression. *Nature* **423**, 655-659, doi:10.1038/nature01576 (2003).

50 Anest, V. *et al.* A nucleosomal function for IkappaB kinase-alpha in NF-kappaB-dependent gene expression. *Nature* **423**, 659-663, doi:10.1038/nature01648 (2003).

51 Jiang, Q., Li, F., Cheng, Z., Kong, Y. & Chen, C. The role of E3 ubiquitin ligase HECTD3 in cancer and beyond. *Cellular and molecular life sciences : CMLS*, doi:10.1007/s00018-019-03339-3 (2019).

52 Li, Y. *et al.* The HECTD3 E3 ubiquitin ligase suppresses cisplatin-induced apoptosis via stabilizing MALT1. *Neoplasia* **15**, 39-48, doi:10.1593/neo.121362 (2013).

53 Li, Y. *et al.* The HECTD3 E3 ubiquitin ligase facilitates cancer cell survival by promoting K63-linked polyubiquitination of caspase-8. *Cell death & disease* **4**, e935, doi:10.1038/cddis.2013.464 (2013).

54 Li, Y. *et al.* The E3 ligase HECTD3 promotes esophageal squamous cell carcinoma (ESCC) growth and cell survival through targeting and inhibiting caspase-9 activation. *Cancer letters* **404**, 44-52, doi:10.1016/j.canlet.2017.07.004 (2017).

55 Cho, J. J. *et al.* Hectd3 promotes pathogenic Th17 lineage through Stat3 activation and Malt1 signaling in neuroinflammation. *Nature communications* **10**, 701, doi:10.1038/s41467-019-08605-3 (2019).

56 Li, F. *et al.* HECTD3 mediates TRAF3 polyubiquitination and type I interferon induction during bacterial infection. *The Journal of clinical investigation* **128**, 4148-4162, doi:10.1172/JCI120406 (2018).

57 Siwko, S. K. *et al.* Lentivirus-mediated oncogene introduction into mammary cells in vivo induces tumors. *Neoplasia* **10**, 653-662, 651 p following 662, doi:10.1593/neo.08266 (2008).

58 Eckhardt, B. L. *et al.* Genomic analysis of a spontaneous model of breast cancer metastasis to bone reveals a role for the extracellular matrix. *Molecular cancer research : MCR* **3**, 1-13 (2005).

59 Srivastava, K. *et al.* Postsurgical adjuvant tumor therapy by combining anti-angiopoietin-2 and metronomic chemotherapy limits metastatic growth. *Cancer cell* **26**, 880-895, doi:10.1016/j.ccell.2014.11.005 (2014).

60 Panigrahy, D. *et al.* Preoperative stimulation of resolution and inflammation blockade eradicates micrometastases. *The Journal of clinical investigation* **129**, 2964-2979, doi:10.1172/JCI127282 (2019).

61 Haupt, W. *et al.* Monocyte function before and after surgical trauma. *Digestive surgery* **15**, 102-104, doi:10.1159/000018601 (1998).

62 Hanahan, D. & Weinberg, R. A. Hallmarks of cancer: the next generation. *Cell* **144**, 646-674, doi:10.1016/j.cell.2011.02.013 (2011).

63 Qian, B. Z. Inflammation fires up cancer metastasis. *Seminars in cancer biology* **47**, 170-176, doi:10.1016/j.semcancer.2017.08.006 (2017).

64 Bouchard, L., Lamarre, L., Tremblay, P. J. & Jolicoeur, P. Stochastic appearance of mammary tumors in transgenic mice carrying the MMTV/c-neu oncogene. *Cell* **57**, 931-936, doi:10.1016/0092-8674(89)90331-0 (1989).

65 Guy, C. T. *et al.* Expression of the neu protooncogene in the mammary epithelium of transgenic mice induces metastatic disease. *Proceedings of the National Academy of Sciences of the United States of America* **89**, 10578-10582, doi:10.1073/pnas.89.22.10578 (1992).

66 Kim, I. S. & Baek, S. H. Mouse models for breast cancer metastasis. *Biochemical and biophysical research communications* **394**, 443-447, doi:10.1016/j.bbrc.2010.03.070 (2010).

67 Liang, H. *et al.* Hypoxia induces miR-153 through the IRE1alpha-XBP1 pathway to fine tune the HIF1alpha/VEGFA axis in breast cancer angiogenesis. *Oncogene* **37**, 1961-1975, doi:10.1038/s41388-017-0089-8 (2018).

68 Huang, W. C. *et al.* Hepatitis B virus X protein induces IKKalpha nuclear translocation via Akt-dependent phosphorylation to promote the motility of hepatocarcinoma cells. *Journal of cellular physiology* **227**, 1446-1454, doi:10.1002/jcp.22860 (2012).

69 Huang, W. C., Ju, T. K., Hung, M. C. & Chen, C. C. Phosphorylation of CBP by IKKalpha promotes cell growth by switching the binding preference of CBP from p53 to NF-kappaB. *Molecular cell* **26**, 75-87, doi:10.1016/j.molcel.2007.02.019 (2007).

70 Temmerman, S. T. *et al.* Defective nuclear IKKalpha function in patients with ectodermal dysplasia with immune deficiency. *The Journal of clinical investigation* **122**, 315-326, doi:10.1172/JCI42534 (2012).

71 Gloire, G. *et al.* Promoter-dependent effect of IKKalpha on NF-kappaB/p65 DNA binding. *The Journal of biological chemistry* **282**, 21308-21318, doi:10.1074/jbc.M610728200 (2007).

72 Cao, Y. *et al.* IKKalpha provides an essential link between RANK signaling and cyclin D1 expression during mammary gland development. *Cell* **107**, 763-775, doi:10.1016/s0092-8674(01)00599-2 (2001).

73 Zandi, E., Chen, Y. & Karin, M. Direct phosphorylation of IkappaB by IKKalpha and IKKbeta: discrimination between free and NF-kappaB-bound substrate. *Science* **281**, 1360-1363, doi:10.1126/science.281.5381.1360 (1998).

74 Woronicz, J. D., Gao, X., Cao, Z., Rothe, M. & Goeddel, D. V. IkappaB kinase-beta: NF-kappaB activation and complex formation with IkappaB kinase-alpha and NIK. *Science* **278**, 866-869, doi:10.1126/science.278.5339.866 (1997).

75 Bonizzi, G. & Karin, M. The two NF-kappaB activation pathways and their role in innate and adaptive immunity. *Trends in immunology* **25**, 280-288, doi:10.1016/j.it.2004.03.008 (2004).

76 Pletz, N. *et al.* Doxorubicin-induced activation of NF-kappaB in melanoma cells is abrogated by inhibition of IKKbeta, but not by a novel IKKalpha inhibitor. *Experimental dermatology* **21**, 301-304, doi:10.1111/j.1600-0625.2012.01440.x (2012).

77 Massague, J. & Obenauf, A. C. Metastatic colonization by circulating tumour cells. *Nature* **529**, 298-306, doi:10.1038/nature17038 (2016).

78 Demicheli, R., Retsky, M. W., Hrushesky, W. J., Baum, M. & Gukas, I. D. The effects of surgery on tumor growth: a century of investigations. *Annals of oncology : official journal of the European Society for Medical Oncology* **19**, 1821-1828, doi:10.1093/annonc/mdn386 (2008).

79 Krall, J. A. *et al.* The systemic response to surgery triggers the outgrowth of distant immune-controlled tumors in mouse models of dormancy. *Science translational medicine* **10**, doi:10.1126/scitranslmed.aan3464 (2018).

80 Sulciner, M. L. *et al.* Resolvins suppress tumor growth and enhance cancer therapy. *The Journal of experimental medicine* **215**, 115-140, doi:10.1084/jem.20170681 (2018).

81 Al-Sahaf, O., Wang, J. H., Browne, T. J., Cotter, T. G. & Redmond, H. P. Surgical injury enhances the expression of genes that mediate breast cancer metastasis to the lung. *Annals of surgery* **252**, 1037-1043, doi:10.1097/SLA.0b013e3181efc635 (2010).

82 Neeman, E., Zmora, O. & Ben-Eliyahu, S. A new approach to reducing postsurgical cancer recurrence: perioperative targeting of catecholamines and prostaglandins. *Clinical cancer research : an official journal of the American Association for Cancer Research* **18**, 4895-4902, doi:10.1158/1078-0432.CCR-12-1087 (2012).

83 Chang, H. Y. *et al.* Robustness, scalability, and integration of a wound-response gene expression signature in predicting breast cancer survival. *Proceedings of the National Academy of Sciences of the United States of America* **102**, 3738-3743, doi:10.1073/pnas.0409462102 (2005).

84 Coffey, J. C. *et al.* Excisional surgery for cancer cure: therapy at a cost. *The Lancet. Oncology* **4**, 760-768, doi:10.1016/s1470-2045(03)01282-8 (2003).

85 Forget, P. *et al.* Do intraoperative analgesics influence breast cancer recurrence after mastectomy? A retrospective analysis. *Anesthesia and analgesia* **110**, 1630-1635, doi:10.1213/ANE.0b013e3181d2ad07 (2010).

86 Lu, Z. *et al.* Epigenetic therapy inhibits metastases by disrupting premetastatic niches. *Nature* **579**, 284-290, doi:10.1038/s41586-020-2054-x (2020).

87 Schumacher, D., Strilic, B., Sivaraj, K. K., Wettschureck, N. & Offermanns, S. Platelet-derived nucleotides promote tumor-cell transendothelial migration and metastasis via P2Y2 receptor. *Cancer cell* **24**, 130-137, doi:10.1016/j.ccr.2013.05.008 (2013).

88 Labelle, M., Begum, S. & Hynes, R. O. Direct signaling between platelets and cancer cells induces an epithelial-mesenchymal-like transition and promotes metastasis. *Cancer cell* **20**, 576-590, doi:10.1016/j.ccr.2011.09.009 (2011).

89 Strell, C., Lang, K., Niggemann, B., Zaenker, K. S. & Entschladen, F. Surface molecules regulating rolling and adhesion to endothelium of neutrophil granulocytes and MDA-MB-468 breast carcinoma cells and their interaction. *Cellular and molecular life sciences : CMLS* **64**, 3306-3316, doi:10.1007/s00018-007-7402-6 (2007).

90 Li, J. & King, M. R. Adhesion receptors as therapeutic targets for circulating tumor cells. *Frontiers in oncology* **2**, 79, doi:10.3389/fonc.2012.00079 (2012).

91 Wu, Q. D., Wang, J. H., Condron, C., Bouchier-Hayes, D. & Redmond, H. P. Human neutrophils facilitate tumor cell transendothelial migration. *American journal of physiology. Cell physiology* **280**,

C814-822, doi:10.1152/ajpcell.2001.280.4.C814 (2001).

92 Schlesinger, M. *et al.* The inhibition of the integrin VLA-4 in MV3 melanoma cell binding by non-anticoagulant heparin derivatives. *Thrombosis research* **129**, 603-610, doi:10.1016/j.thromres.2011.10.023 (2012).

93 Hoberg, J. E., Popko, A. E., Ramsey, C. S. & Mayo, M. W. IkappaB kinase alpha-mediated derepression of SMRT potentiates acetylation of RelA/p65 by p300. *Molecular and cellular biology* **26**, 457-471, doi:10.1128/MCB.26.2.457-471.2006 (2006).

94 Hoberg, J. E., Yeung, F. & Mayo, M. W. SMRT derepression by the IkappaB kinase alpha: a prerequisite to NF-kappaB transcription and survival. *Molecular cell* **16**, 245-255, doi:10.1016/j.molcel.2004.10.010 (2004).

95 Armache, A. *et al.* Histone H3.3 phosphorylation amplifies stimulation-induced transcription. *Nature* **583**, 852-857, doi:10.1038/s41586-020-2533-0 (2020).

96 Colomer, C. *et al.* IKKalpha Kinase Regulates the DNA Damage Response and Drives Chemo-resistance in Cancer. *Molecular cell* **75**, 669-682 e665, doi:10.1016/j.molcel.2019.05.036 (2019).

97 Yamaguchi, T., Miki, Y. & Yoshida, K. Protein kinase C delta activates IkappaB-kinase alpha to induce the p53 tumor suppressor in response to oxidative stress. *Cellular signalling* **19**, 2088-2097, doi:10.1016/j.cellsig.2007.06.002 (2007).

98 Yan, B. *et al.* Activation of AhR with nuclear IKKalpha regulates cancer stem-like properties in the occurrence of radioresistance. *Cell death & disease* **9**, 490, doi:10.1038/s41419-018-0542-9 (2018).

99 Kwak, Y. T. *et al.* IkappaB kinase alpha regulates subcellular distribution and turnover of cyclin D1 by phosphorylation. *The Journal of biological chemistry* **280**, 33945-33952, doi:10.1074/jbc.M506206200 (2005).

Figures

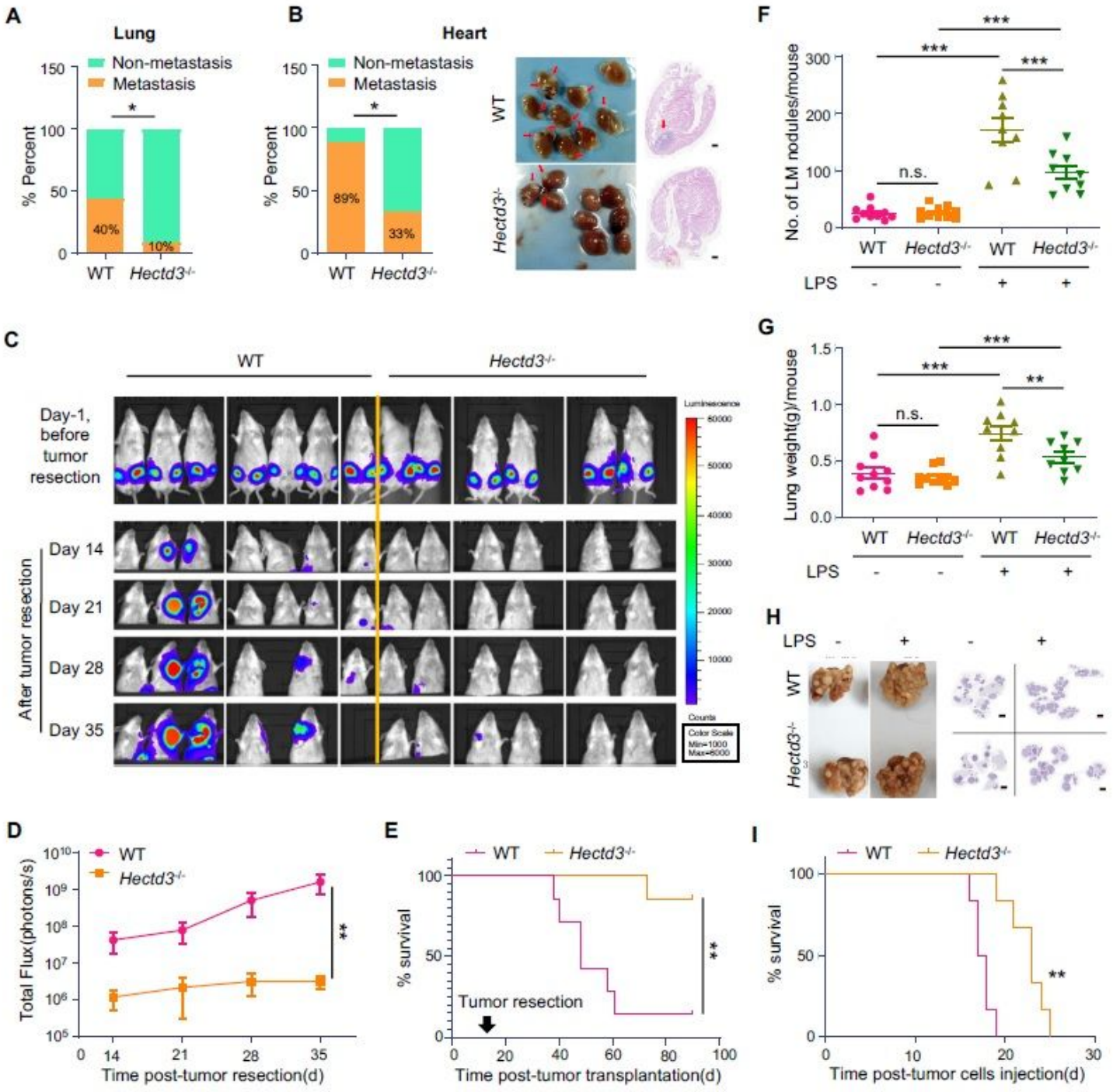

Figure 1

Hectd3 knockout inhibits inflammation-induced tumor metastasis in mice A. A comparison of the incidence of lung metastases in WT (n=9) versus Hectd3-/- (n=11) mice with an FVB genetic background. PyMT-induced tumor cells were orthotopically injected into the fat pad of both groups of mice (5×105 cells per mouse). Primary tumors were removed 20 days later. Mice were sacrificed after 2 months, and the incidence of lung metastasis was recorded. B. PyMT-induced breast tumor cells were inoculated as described above. The incidence of heart metastasis (left), representative heart metastasis nodule images and H&E staining (right) are shown. C. 4T1-Luc2 cells were injected orthotopically into the fat pads of WT

(n=7) and Hectd3-/- (n=6) BALB/c mice (1×105 cells per mouse). Primary tumors were removed 12 days later. Representative bioluminescence images are shown. D. Quantification of bioluminescence signals from panel C. E. Kaplan-Meier survival curves of WT (n=7) and Hectd3-/- (n=6) mice after 4T1-Luc2 cell orthotopic allograft transplantation. 4T1-Luc2 primary tumors were removed 12 days after transplantation. F. WT and Hectd3-/- FVB mice were intravenously injected with or without LPS (1 mg/kg). Five hours later, PyMT-induced breast tumor cells were injected into the tail vein (2×105 cells per mouse). Each group contained 9 to 10 mice, and mice were sacrificed 20 days after injection of tumor cells. The graph shows the number of pulmonary metastasis nodules in each group of mice. G. The weight of the whole lung with metastatic nodules in each group of mice from panel F. H. Representative lung metastasis nodule images and corresponding H&E staining of the lungs in different groups of mice from panel F. I. Kaplan-Meier survival curves of WT (n=6) mice and Hectd3-/- (n=6) mice pretreated with LPS and transplanted with PyMT-induced breast tumor cells. Data are presented as the mean±SEM, and statistics were calculated using the Chi-square test for A and B, two-way ANOVA for D, two-tailed t-test for F and G, and log-rank test for E and I. *, $P<0.05$; **, $P<0.01$; ***, $P<0.001$; n.s., not significant. Scale bars are 500 μm for B and 2 mm for H.

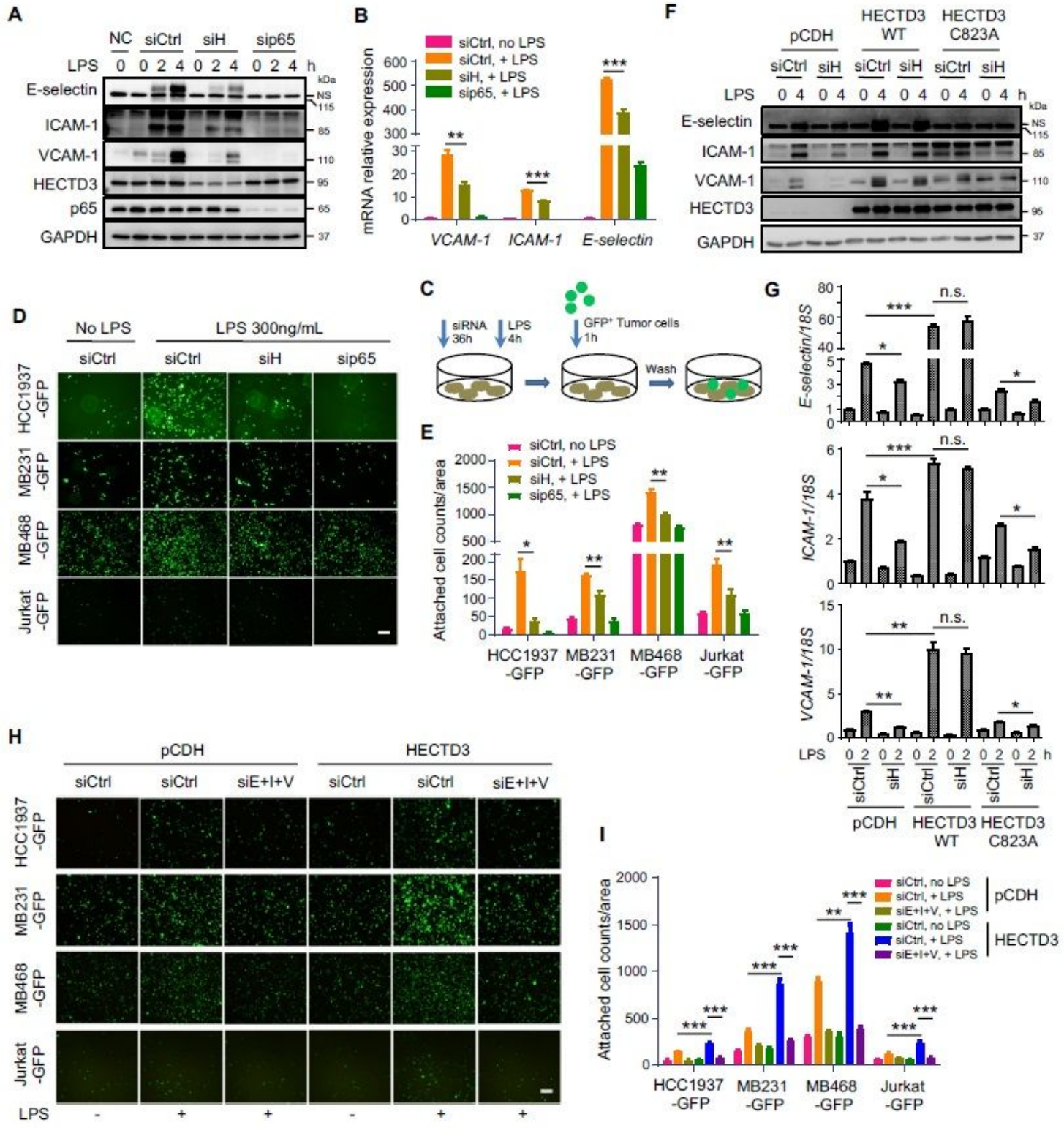

Figure 2

HECTD3 promotes adhesion of tumor cells to HUVECs by upregulating E-selectin, ICAM-1 and VCAM-1 expression in HUVECs A. Immunoblot analysis of adhesion molecules, like E-selectin, ICAM-1 and VCAM-1 in HUVECs knocking down HECTD3 or p65 using corresponding siRNA for 36h, and stimulated with or without LPS (300ng/mL) as indicated time. siControl (siCtrl) targeted nothing and siHECTD3 (siH) was a siRNA pool containing siHECTD3 1# and 2# here and in the following experiments. NC, negative control.

NS, nonspecific band. B. qRT-PCR analysis of adhesion molecules in HUVECs knocking down HECTD3 or p65 and stimulated with LPS (300ng/mL) for 2h. C. Schematic representation of the in vitro adhesion assay. HECTD3 or p65 was knocked down in HUVECs, and cells were seeded into 6-well plates. HUVECs were treated with LPS (300 ng/ml) for 4 h when the cells became fully confluent. Then, suspended GFP-labeled tumor cells were added and incubated for 1 h. Unattached cancer cells were washed away, and cancer cells adhered to HUVECs were quantified. D. Representative images of the adhesion of GFP-labeled tumor cells to monolayer-cultured HUVECs transfected with the indicated siRNA and stimulated with or without LPS. E. Bar graphs show the number of GFP-labeled tumor cells attached to monolayer-cultured HUVECs. F. HUVECs stably overexpressing siRNA-resistant HECTD3, HECTD3 C823A mutant, and control (pCDH) were established. Immunoblots of these HUVECs knocked down endogenous HECTD3 or not and stimulated with LPS (300 ng/ml) for 4 h. G. HUVECs stably overexpressing siRNA-resistant HECTD3, HECTD3 C823A mutant, and control (pCDH) were established. qRT-PCR analysis of these HUVECs knocked down endogenous HECTD3 or not and stimulated with LPS (300 ng/ml) for 2 h. H. Representative images of the adhesion of GFP-labeled tumor cells to monolayer-cultured HUVECs in which HECTD3 was overexpressed or not. E-selectin, ICAM-1 and VCAM-1 were simultaneously knocked down by siE+I+V, a siRNA mixture of siE-selectin, siICAM-1 and siVCAM-1. I. Quantitative data of panel H. Data are presented as the mean±SEM, and statistics were calculated using a two-tailed t-test for B, E, G and I. *, $P<0.05$; **, $P<0.01$; ***, $P<0.001$; n.s., not significant. Scale bars, 200 μm for D and H.

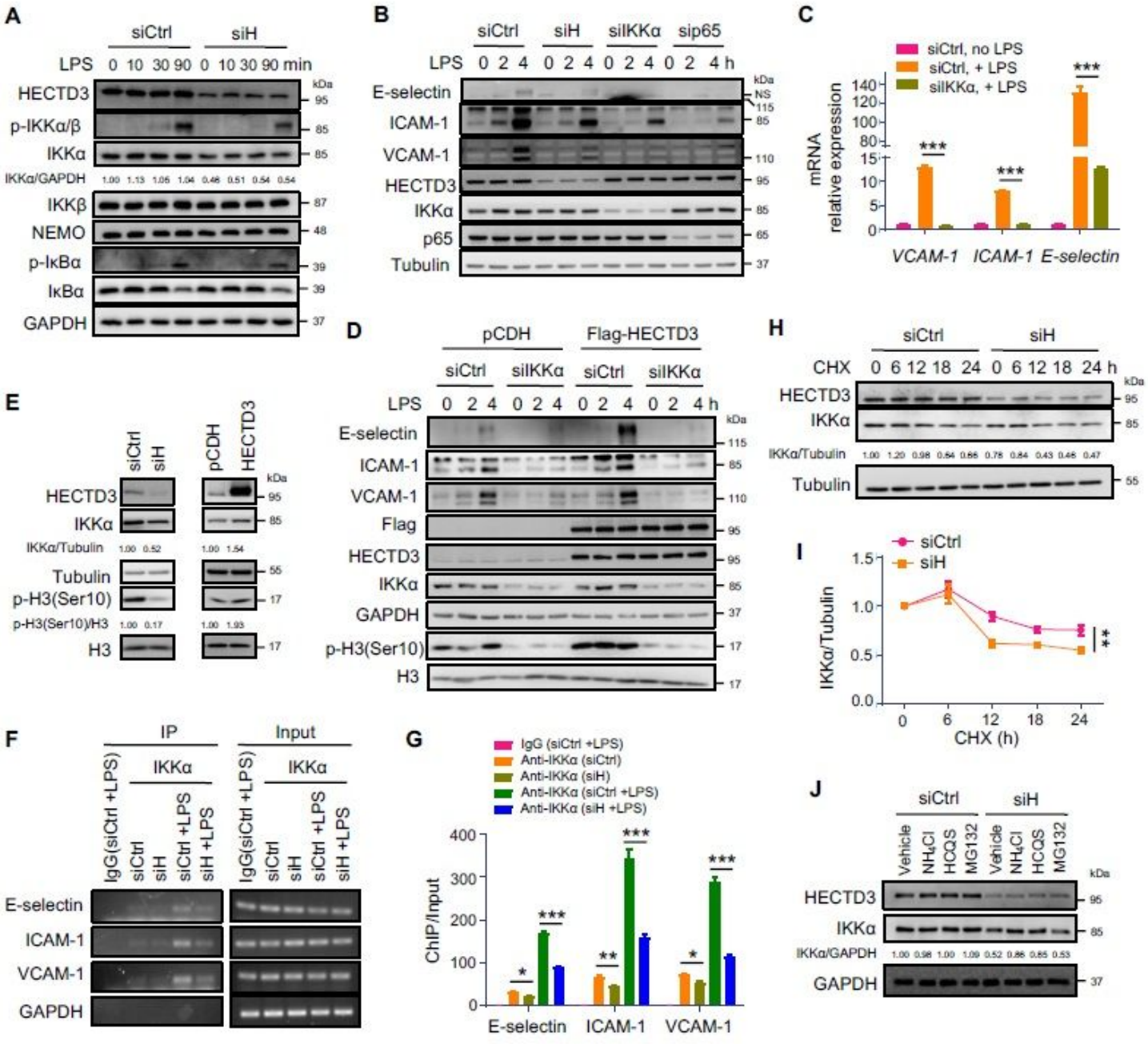

Figure 3

HECTD3 increases the expression of adhesion molecules by stabilizing IKKa and recruiting nuclear IKKa to adhesion molecule gene promoters A. Immunoblot analysis of the expression of IKKα and activation degree of the NF-κB signal pathway. HUVECs knocking down HECTD3 were stimulated with LPS (300 ng/ml) for indicated time. B. A comparison of the expression of the adhesion molecules in HUVEC knocking down HECTD3, IKKα and p65, and stimulated with or without LPS(300ng/mL) as indicated time. C. qRT-PCR analysis of adhesion molecules in HUVECs knocking down IKKα and stimulated with or without LPS (300ng/mL) for 2 hours . D. IKKa was transiently knocked down in HECTD3-overexpressing HUVECs. LPS (300 ng/ml) and HECTD3 overexpression-induced increases in adhesion molecule

expression were blocked when IKKa was depleted. E. HECTD3 positively regulated IKKa and p-H3(Ser10) levels in HUVECs. Left: HECTD3 was knocked. Right: HECTD3 was stably overexpressed in HUVECs. F. Chromatin immunoprecipitation (ChIP) assays were performed using an anti-IKKa antibody in HUVECs transfected with siControl or siHECTD3 and stimulated with LPS (300 ng/mL) for 2 h. G. qPCR results of the samples in panel F. H. HECTD3 knockdown by siRNA decreased IKKaprotein stability in HUVECs. The cells were incubated with 50 μg/ml CHX for the indicated times and were collected for immunoblotting. Tubulin was used as the internal control. The band intensity of IKKa at each time point was quantified using ImageJ. The experiments were repeated three times, and a representative experimental result is presented. I. Quantitative data of panel H. J. HECTD3 knockdown induced IKKa protein degradation through lysosomes but not proteasomes. HUVECs were treated with lysosome inhibitors (NH4Cl, 10 mM and HCQS, 50 μM, overnight) or proteasome inhibitor (MG132, 20 μM for 6 h) after knocking down HECTD3. Data are presented as the mean±SEM, and statistics were calculated using two-tailed t-test for C and F, two-way ANOVA for I. *, P<0.05; **, P<0.01; ***, P<0.001.

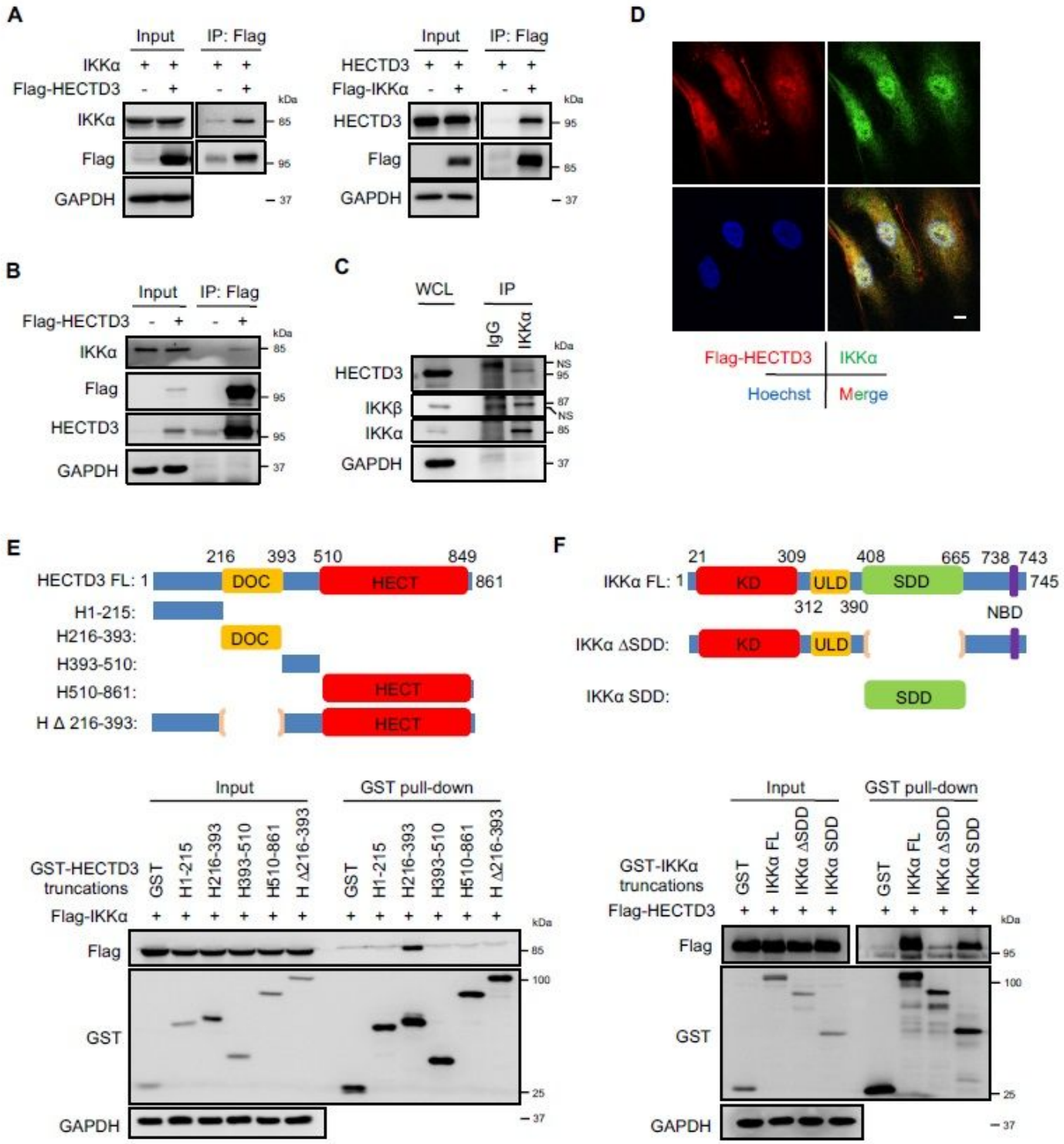

Figure 4

HECTD3 interacts with IKKα A. Exogenous HECTD3 interacts with IKKα in HEK293T cells. Flag-HECTD3 and IKKa (left) or Flag-IKKa and HECTD3 (right) plasmids were cotransfected into HEK293T cells. After Flag-tagged HECTD3 and IKKa proteins were immunoprecipitated with Flag-M2 beads, IKKa and HECTD3 were detected by immunoblotting. B. FLAG-immunoprecipitation of FLAG-tagged HECTD3 from HUVECs. C. Anti-IKKa antibody was used to immunoprecipitate IKKa from HUVECs. D. Confocal microscopy

images of Flag-HECTD3 and IKKα in HUVECs are shown. Scale bars, 10 μm. E. Schematic diagram shows human HECTD3 and its truncation mutants (top). Flag-IKKa and GST-fused HECTD3 truncation mutants were coexpressed in HEK293T cells. By GST pull-down assay (bottom), GST-H216-393 specifically pulled down Flag-IKKa. F. Schematic diagram shows human IKKa and its truncation mutants (top). Flag-HECTD3 and GST-fused IKKa truncation mutants were coexpressed in HEK293T cells. By the GST pull-down assay (bottom), GST-IKKaSDD specifically pulled down Flag-HECTD3.

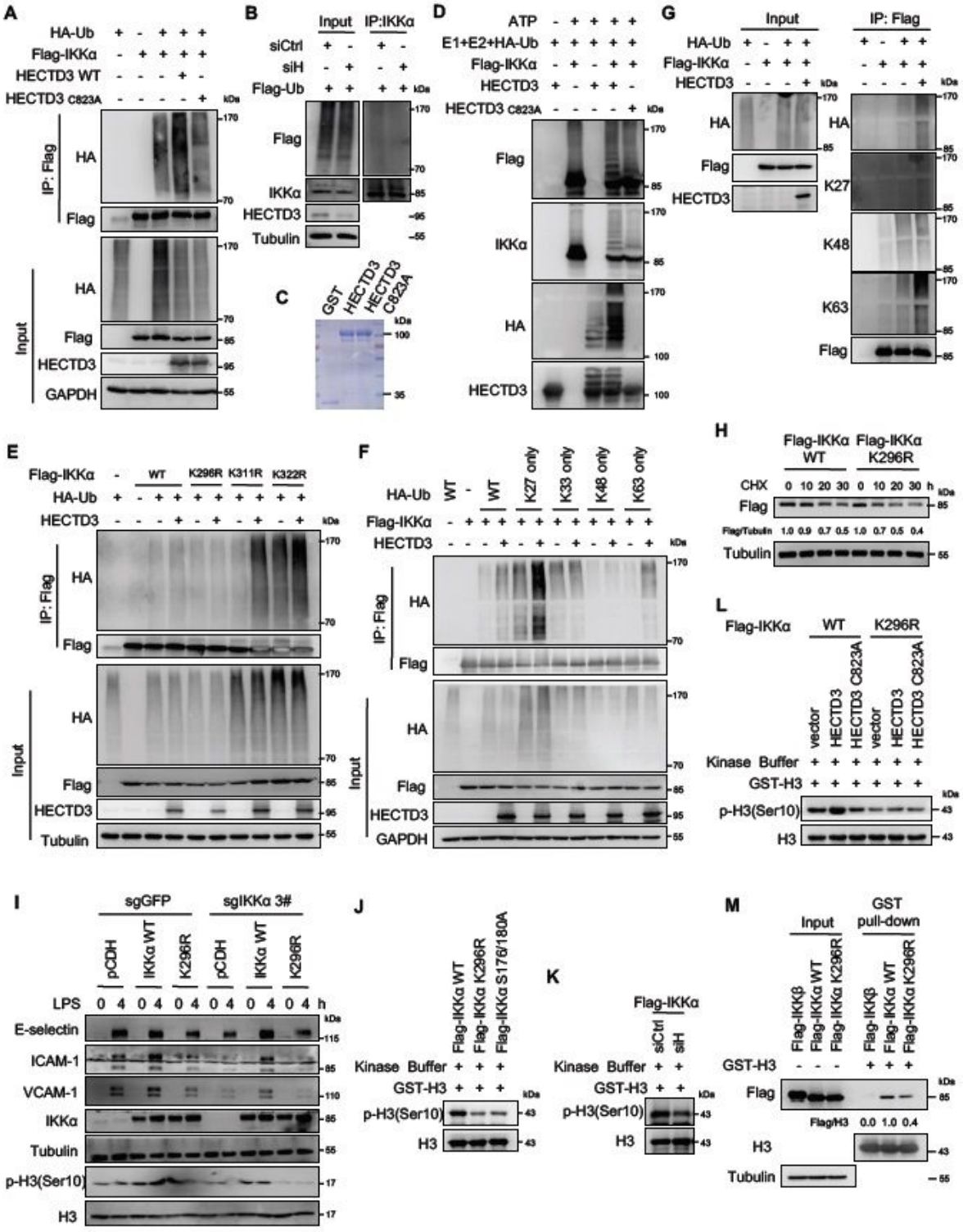

Figure 5

HECTD3 ubiquitinates IKKa with K27- and K63-linked polyubiquitin chains at K296 and increases IKKa protein stability and kinase activity A. Flag–IKKa, HA–Ub, and HECTD3 (WT) or HECTD3 C823A were coexpressed in HEK293T cells. Ubiquitinated Flag–IKKa proteins were immunoprecipitated with Flag-M2 beads and probed with anti-HA antibody. B. Co-IP analysis of the ubiquitination of endogenous IKKα in HUVECs overexpressing stable Flag-ubiquitin (Flag-Ub). The cells were transfected with siRNA to knock down HECTD3. Anti-IKKα antibody was used for immunoprecipitation. The anti-Flag antibody was used to detect ubiquitinated IKKa. C. Purified recombinant HECTD3 and HECTD3 C823A proteins from E. coli were detected by Coomassie blue staining. D. HECTD3 ubiquitinates IKKa in vitro in an E3 ligase activity-dependent manner. ATP, HA-Ub, E1, UbcH5b, HECTD3 or HECTD3 C823A, and Flag-IKKa were mixed for ubiquitination assays. The Flag-IKKα protein was purified from HEK293 cells transfected with the plasmid encoding Flag-IKKausing Flag-M2 beads. E. HECTD3 ubiquitinates IKKa at K296. HECTD3 failed to ubiquitinate Flag-IKKaK296R, similar to WT, K311R and K322R in HEK293T cells. F. HECTD3 ubiquitinates IKKawith K27- and K63-linked polyubiquitin chains. WT, K27 only, and K63 only HA-Ub supported HECTD3-mediated Flag-IKKa ubiquitination. In contrast, K33 only and K48 only HA-Ub failed to do so. G. Linkage-specific antibodies were used to validate the linkage of Flag-IKKa. H. CHX chase assays were used to analyze the half-lives of Flag-IKK WT and K296R mutant in HEK293T cells. I. IKKa ubiquitination at K296 is essential for LPS to induce adhesion molecule expression in HUVECs. IKKa was stably knocked out in HUVECs using the CRISPR/Cas9 system. Immunoblotting of adhesion molecule expression in these cells restored the expression of IKKα by lentivirus encoding Flag-IKKα WT or Flag-IKKα K296R and stimulated with or without LPS (300 ng/mL) for indicated time (0-4 h). J. The in vitro IKKa kinase assay contains purified Flag-IKKα WT, K296R, S175/180A, GST-H3, and ATP. Flag-IKKa proteins were purified from HEK293T cells. K. HECTD3 knockdown decreased IKKa activity toward histone H3. HECTD3 knockdown and Flag-IKKα overexpression were performed in HEK293T cells. Flag-IKKα proteins were purified for in vitro kinase assays toward GST-H3. L. Overexpression of HECTD3, not HECTD3 C823A, increased IKKa activity toward histone H3. Flag-IKKα and Flag-IKKα K296R proteins were purified from HEK293T cells cotransfected with plasmids encoding Flag-IKKα or Flag-IKKα K296R with HECTD3 or HECTD3 C823A. In vitro kinase assays of Flag-IKKα WT and Flag-IKKα K296R toward GST-H3 were performed. M. Flag-IKKa K296R decreased the interaction with H3 compared to Flag-IKKa WT. Cell lysates of HEK293T cells expressing Flag-IKKα WT or Flag-IKKα K296R were collected and incubated with purified GST-H3 protein for 30 min on ice. The GST pull-down assay was performed using glutathione sepharose beads.

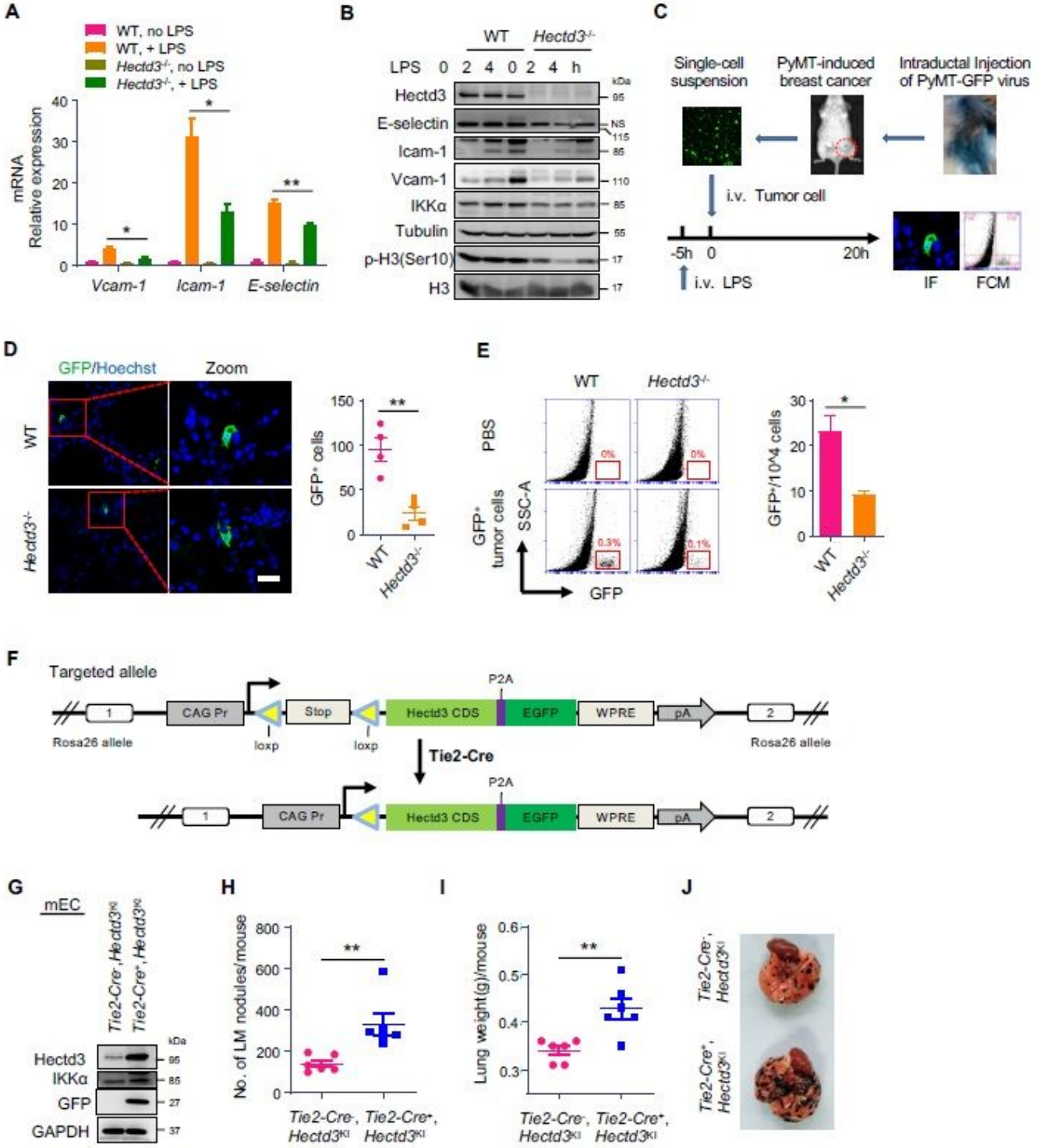

Figure 6

Hectd3 promotes the adhesion of tumor cells to mouse lung vascular endothelial cells through IKKa under inflammatory conditions A. qRT-PCR analysis of adhesion molecules in WT and Hectd3 KO mECs stimulated with LPS (500 ng/ml) for 2 h. B. A comparison of the expression of the adhesion molecules, IKKα and p-H3(Ser10) in mECs stimulated with or without LPS (500ng/mL) as indicated time. C. Schematic representation of the in vivo adhesion assay. 1) Lentiviruses overexpressing PyMT and GFP

were injected intraductally to induce breast tumors. 2) Tumor cells were digested into a single-cell suspension. 3) The single-cell suspension (5×106 cells per mouse) was injected through the tail vein into WT or Hectd3-/- mice pretreated with LPS (1 mg/kg) stimulation for 5 h. 4) Twenty hours after tumor cell injection, the mice were sacrificed and perfused to analyze tumor cell colonization in the lungs. D. Representative frozen immunofluorescence images of GFP+ tumor cells in lungs of mice from C (left) and bar graph showing the number of GFP+ tumor cells in lungs of WT and Hectd3-/- mice (right). Counting rules: Eighty sections were randomly cut from each sample (the entire lung) and then scanned by a Fluo View FV1000 confocal microscope after fluorescence staining. The total number of GFP-positive tumor cells in 80 sections was recorded. E. The lungs of WT and Hectd3-/- mice from C were digested completely with collagen I. GFP+ tumor cells were analyzed by flow cytometry (left) and quantified (right). F. Schematic representation of the targeted allele and the conditional allele of Hectd3 KI. G. The protein expression of Hectd3, IKKa and GFP in mECs isolated from the lungs of Tie2-Cre-;Hectd3KI and Tie2-Cre+;Hectd3KI mice was detected by immunoblotting. H. B16-F10 cells were injected by tail vein into Tie2-Cre-;Hectd3Ki and Tie2-Cre+;Hectd3KI mice (1×105 per mouse,6 mice/group) which were pretreated with LPS (1mg/kg) intravenous injection for 5 hours. The mice were sacrificed 20 days after the injection of cancer cells. The number of pulmonary metastasis nodules in each group of mice is shown. I. Analysis of the weight of whole lung with metastasis nodules in each group mice from H. J. Representative lung metastasis nodule images in each group mice from H. Data are presented as the mean±SEM, and statistics were calculated using a two-tailed t-test for A, D, E, H and I. *, $P<0.05$; **, $P<0.01$; ***, $P<0.001$. Scale bars, 100 μm for D.

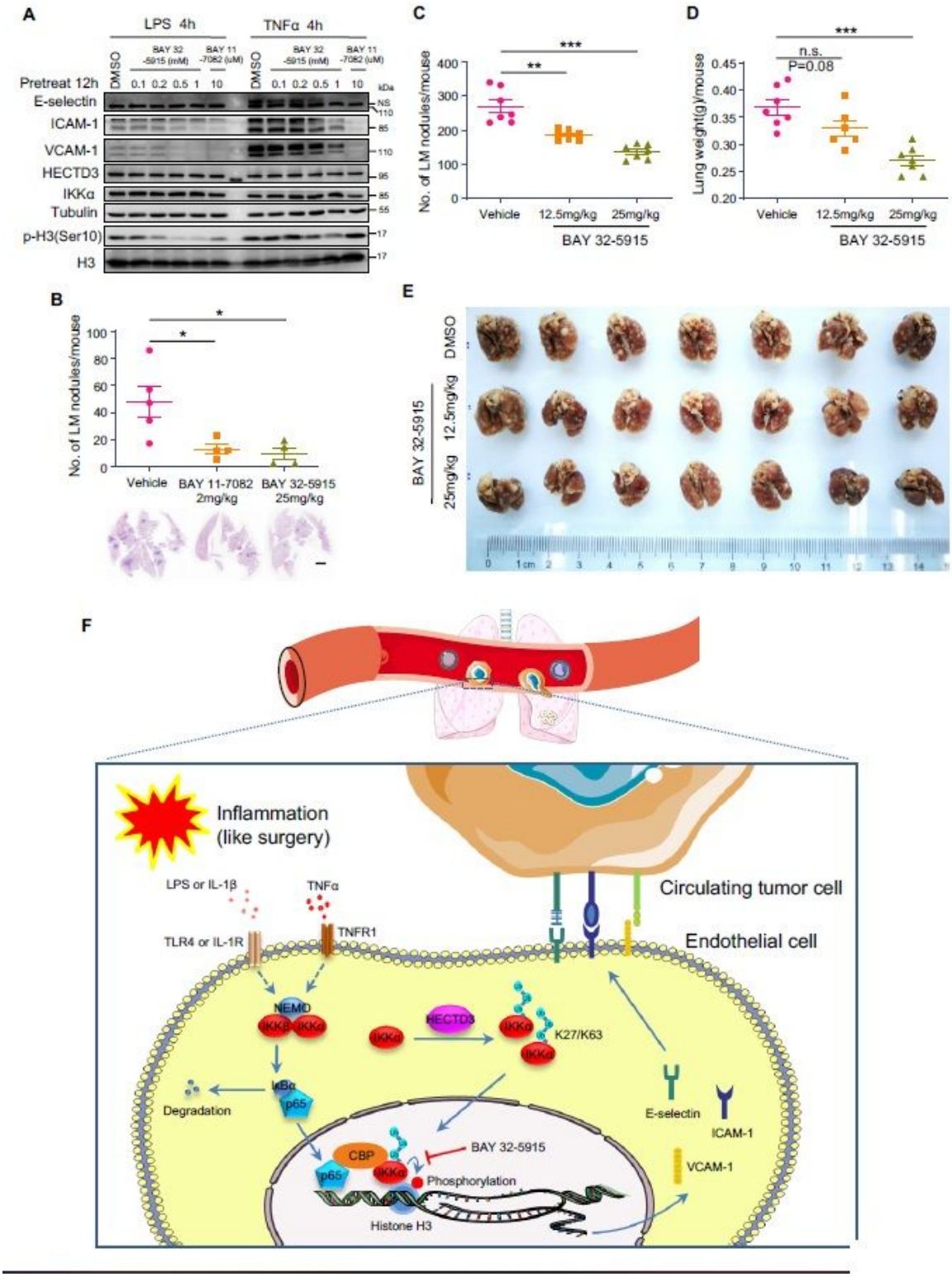

Figure 7

BAY 32-5915, an IKKα-specific kinase inhibitor, suppresses tumor lung metastasis. A. Immunoblot analysis of the expression of adhesion molecules in HUVECs pretreated with specific IKKα kinase inhibitor BAY 32-5915 as indicated concentration for 12 hours, DMSO as a negative control and BAY 11-7082(10μM) as a positive control, followed by treatment of LPS (300ng/mL) or TNFα (10ng/mL) for 4 hours. B. 4T1-Luc2 cells were injected by tail vein into BALB/c mice (1×105 per mouse) that were

pretreated with vehicle, BAY 32-5915 (25 mg/kg) or BAY 11-7082 (2 mg/kg) for 24 h and LPS (1 mg/kg) for 5 h by intravenous injection. The mice were sacrificed 16 days after the injection of tumor cells. The number of mouse pulmonary metastasis nodules in the three groups is shown. Representative H&E staining images from each group are shown below the graph. C. PyMT-induced breast tumor cells were injected by tail vein into FVB mice (2×105 per mouse) that were pretreated with vehicle, BAY 32-5915 (12.5 mg/kg) or BAY 32-5915 (12.5 mg/kg) for 24 h and LPS (1 mg/kg) for 5 h by intravenous injection. The mice were sacrificed 20 days after the injection of tumor cells. The number of mouse pulmonary metastasis nodules in the three groups is shown. D. Analysis of the weight of whole lung with metastasis nodules in the three groups from C. E. Representative lung metastasis nodule images of the lungs in the three groups from C. F. The hypothetical working model. Inflammatory factors, including LPS, TNFa, and IL-1β, activate the NF-aB pathway and promote p65 nuclear translocation and transcription of adhesion molecules, including E-selectin, ICAM-1 and VCAM-1, in HUVECs. HECTD3 ubiquitinates IKKa with K27/K63-linked polyubiquitin chains at K269 to increase IKKa protein stability, kinase activity, and recruitment to NF-a B-responsive gene promoters, where IKKa phosphorylates histone H3 at Ser10 to increase the transcription of adhesion molecules. These adhesion molecules on the EC plasma membrane promote the adhesion of tumor cells to the endothelium, leading to extravasation, colonization and metastasis. IKKa and HECTD3-specific inhibitors may prevent cancer metastasis. Data are presented as the mean±SEM, and statistics were calculated using a two-tailed t-test for B, C and D. *, P<0.05; **, P<0.01; ***, P<0.001; n.s., not significant. Scale bars, 2 mm for B.

Supplementary Files

This is a list of supplementary files associated with this preprint. Click to download.

- SI12162020.docx
- SupplementalFiguresHECTD3metastasis3.pdf